
Chapter 7
Radiolabeling,
Biodistribution and
Blood Clearance studies

CHAPTER-7 RADIOLABELING, BIODISTRIBUTION AND BLOOD CLEARANCE STUDIES

7.1 Introduction

Radiolabeling is incorporation of a radioactive element into a compound. Radiolabeling studies on drugs and drug delivery systems have recently gained importance for studying their biodistribution and their fate in the body.

The use of nuclear medicine applications in oncology is of particular importance as a rapidly developing therapeutic and diagnostic multimodality. Numerous investigations have shown that incorporating anticancer agents in nanoparticulate carriers would provide a useful means for controlling the cellular distribution profiles of these agents. The rationale behind these approaches is to combine a drug controlled release fashion with a targeted delivery in order to provide more efficient and less harmful solutions, thus, surmounting the limitations often encountered in conventional chemotherapy (Brigger et al., 2002).

Radionuclide imaging is commonly of two types; single photon emission computed tomography (SPECT) and positron emission tomography (PET). Generally, typical imaging studies include dynamic or static imaging and in vivo function tests. Dynamic imaging provides clinicians with necessary data about biological turnover of radioisotopes in different body compartments and organs. Single-photon radionuclides emit gamma (γ) rays in the energy range of approximately 75 to 360 keV (Coleman et al., 2003). Examples of these radionuclides include: ^{131}I , ^{67}Ga , ^{111}In , ^{123}I and $^{99\text{m}}\text{Tc}$. Technetium-99m is so far the most commonly used radionuclide in nuclear imaging. More than 80% of all usually used radiopharmaceuticals contain this short-lived metastable radionuclide (Banerjee et al., 2001). This is due to the highly interesting physical properties of $^{99\text{m}}\text{Tc}$ among which its short half-life (6 h) and gamma photon emission of 140 keV, which is advantageous for both effective imaging and patient safety perspectives. Technetium-99m can be derived as a column elute from a $^{99}\text{Mo}/^{99\text{m}}\text{Tc}$ generator which makes it readily available. Furthermore, $^{99\text{m}}\text{Tc}$ possesses latent chemical properties; facilitating thereby the labelling of several types of kits for versatile

diagnostic applications. Apart from ^{99m}Tc , other commonly used γ -emitters are Indium-111 (^{111}In), Iodine-123 (^{123}I) and Gallium-67 (^{67}Ga) (Dietlein et al., 2005).

Nanoparticles prepared from poly(alkylcyanoacrylate) labeled with ^{99m}Tc and ^{111}In have been described for cancer imaging in clinical studies. Ghanem et al. labelled poly(isobutyl and isohexyl cyanoacrylate) nanoparticles with ^{99m}Tc and ^{111}In by using an isotope chelated with diethylene triamine penta acetic acid (DTPA) as a spacer to fix the radioisotopes (Ghanem et al., 1993). This system yielded a labelling efficiency of more than 80% and was relatively stable during the whole period of investigation. However, 60–75% of nanoparticles were detected in the RES organs of rabbits as it was shown by gamma camera images. Other researchers described the labelling of chitosan nanoparticles with ^{99m}Tc using stannous chloride to reduce the pertechnetate ions. Yet again, the biodistribution of radiolabelled nanoparticles revealed localization of the radioactivity mainly in both the liver and the spleen (Douglas et al., 1986).

In the present study, we carried out radiolabeling of pure drugs and their formulations (ETO, ETO-PLGA NP, ETO-PLGA-PLU NP, ETO-PLGA-MPEG NP, CYT, CYT-PLGA NP and CYT-PLGA-MPEG NP) using ^{99m}Tc . After checking their labeling efficiency and stability, the formulations were studied for biodistribution in mice and blood clearance in rats.

7.2 Materials

Table 7.1
List of materials

Material	Source/Manufacturer
Etoposide, Cytarabine	Gift samples from Biocon, Bangalore
Poly (DL lactide-co-glycolide) PLGA 50:50 (inherent viscosity 0.22 dl/g)	Gift sample from Boehringer Ingelheim Limited, Germany
Pluronic F-68 (BASF)	Gift sample from Alembic Ltd, Vadodara.
Technetium-99m (^{99m} Tc) as Pertechnetate (TcO ₄ ⁻) Regional Center for Radiopharmaceutical division (Northern region), Board of Radiation and Isotope Technology, Delhi, India	Kindly supplied by INMAS, Delhi
Stannous chloride	Kindly supplied by INMAS, Delhi
Acetic acid	Kindly supplied by INMAS, Delhi
Sodium bicarbonate	Kindly supplied by INMAS, Delhi
Chloroform, AR grade	SD Fine Chemicals, Mumbai
Methanol, AR grade	SD Fine Chemicals, Mumbai
Acetone, AR grade	SD Fine Chemicals, Mumbai
Silica gel coated fibre sheets (Gelman Sciences Inc., Ann Arbor, MI)	Kindly supplied by INMAS, Delhi
Sodium Chloride	SD Fine Chemicals, Mumbai

Animals

Balb/c mice of either sex weighing 20-25 g and Sprague-Dawley rats of either sex weighing 200-250 g were obtained from INMAS, Delhi. All animal experiments were approved and carried out as per Institutional Animal Ethics Committee's Guidelines, INMAS, Delhi.

SECTION A-RADIOLABELING STUDIES

7.3 Radiolabeling of formulations

Etoposide, ETO-PLGA NP, ETO-PLGA-mPEG NP, Cytarabine, CYT-PLGA NP were radiolabeled with Technetium-99m (^{99m}Tc) as per method described by Theobald (1990). Briefly, the pertechnetate (TcO_4^-) (2 mCi) was reduced with stannous chloride (in 10% acetic acid) and the pH was adjusted to 6.5 with 0.5M sodium bicarbonate. To it was added the test formulation to be radiolabeled in a concentration of 1mg/ml and incubated at room temperature for 10 minutes and checked for labeling efficiency and stability before injecting in the animals.

7.4 Labeling efficiency and colloid formation

The labeling efficiency of the ^{99m}Tc labeled drug and NP was determined by instant thin layer chromatography (ITLC) using ITLC-SG mini strips as described by Banerjee et al. (2005). Silica gel coated fibre sheets were used for ascending thin layer chromatography. 1-2 μl of labeled complex was put at the bottom of the strip and acetone was used as the mobile phase. The solvent front was allowed to reach up to height of 7cm from the origin and was then cut into two halves. Radioactivity was checked in each half by gamma ray spectrometer (GRS23C, Electronics Corporation of India Limited, India). Colloid formation was determined in solvent. The radiocolloids would remain at the bottom of the strip, while free pertechnetate and labeled complex would migrate to the solvent front. The actual amount of drug labeled and nanoparticle labeled ^{99m}Tc was calculated by subtracting the migrated activity with the solvent front using acetone: 0.9% saline mixture (1:1).

7.5 Stability of the ^{99m}Tc Labeled Complexes

The stability of labeled complexes in serum supports their stability in biological environment upon administration into the body. The stability of ^{99m}Tc labeled complexes of the test formulations (drugs and NPs) was determined in vitro in human serum by ascending ITLC technique (Reddy et al., 2004). The labeled complex (0.1ml) was incubated with freshly collected human serum (0.4ml) at 37°C. The stability was performed by determining the changes in labeling efficiency at regular intervals up to 24

h and analyzing the chromatograms in gamma ray spectrometer (GRS23C, Electronics Corporation of India Limited, India)

7.6 Results and discussion of radiolabeling studies

7.6.1 Etoposide and etoposide loaded nanoparticles

Etoposide and etoposide loaded PLGA nanoparticles were labeled with ^{99m}Tc using ITLC-Silica Gel as the stationary phase and acetone: 0.9% saline (1:1) as mobile phase. Pertecchneate exists in an oxidative state and hence was reduced to its lower valence state by the use of stannous chloride and the pH was adjusted to 6.5-7.0. Amount of stannous chloride plays an important role in the labeling efficiency; the effect of amount of stannous chloride on the labeling efficiency of Etoposide is shown in Table 7.2a. The optimum amount of stannous chloride resulting in high labeling efficiency and low amount of radiocolloids was found to be 50 μg . 99.32 % labeling efficiency of etoposide was achieved with a low amount of 0.13% formation of colloids. Increasing the concentration above 50 μg not only decreased labeling efficiency but also increased colloid formation. Table 7.2b show the effect of amount of stannous chloride on the labeling efficiency of etoposide loaded PLGA NPs: Eto-PLGA NP₁₀₅ (etoposide loaded PLGA nanoparticles with mean particle size of 105nm) and Eto-PLGA NP₁₆₀ (etoposide loaded PLGA nanoparticles with mean particle size of 160nm). A similar pattern was followed in the labeling efficiency in the labeling of NPs as well. 75 μg of stannous chloride was found to be optimum for both the etoposide loaded PLGA NPs resulting in a high labeling efficiency of 99.03 and 98.32% for Eto-PLGA NP₁₀₅ and Eto-PLGA NP₁₆₀ respectively. There was no significant ($p>0.05$) difference between labeling efficiency of Eto-PLGA NP₁₀₅ and Eto-PLGA NP₁₆₀. Table 7.2c show the effect of amount of stannous chloride on the labeling efficiency of etoposide loaded PLGA-PLURONIC nanoparticles (Eto-PLGA-PLU NP) and etoposide loaded PLGA-MPEG nanoparticles (Eto-PLGA-MPEG NP). 100 μg of stannous chloride was found to be optimum for both the etoposide loaded PLGA NPs resulting in a high labeling efficiency of 98.39 and 99.38 % for Eto-PLGA-PLU NP and Eto-PLGA-MPEG NP respectively. There was no significant ($p>0.05$) difference between labeling efficiency of Eto-PLGA-PLU NP and Eto-PLGA-MPEG NP.

Table 7.2a
Effect of amount of stannous chloride on the labeling efficiency of etoposide

Stannous Chloride (μg)	Etoposide		
	% Labeled	% Colloids	% Free
25	83.19	5.98	10.9
50	99.32	0.13	0.05
75	95.19	3.59	1.22
100	93.15	2.45	4.4
125	92.09	4.71	3.2
150	91.06	5.45	3.49

Table 7.2b
Effect of amount of stannous chloride on the labeling efficiency of etoposide loaded NPs.

Stannous Chloride (μg)	Eto-PLGA NP ₁₀₅ (ENP5)			Eto-PLGA NP ₁₆₀ (ENP2)		
	% Labeled	% Colloids	% Free	% Labeled	% Colloids	% Free
25	89.16	7.02	3.82	87.14	5.02	7.80
50	98.42	1.42	0.16	96.48	1.40	2.10
75	99.03	0.44	0.43	98.32	0.12	1.54
100	94.19	4.12	1.69	92.15	2.12	5.70
125	92.14	6.41	1.45	90.13	4.45	5.40
150	90.48	7.12	2.40	89.42	5.10	5.44

Eto-PLGA NP₁₀₅ (ENP5) refers to etoposide loaded PLGA nanoparticles with mean particle size of 105nm and Eto-PLGA NP₁₆₀ (ENP2) refers to etoposide loaded PLGA nanoparticles with mean particle size of 160nm.

Table 7.2c
Effect of amount of stannous chloride on the labeling efficiency of Etoposide loaded PLGA Nanoparticles

Stannous Chloride (µg)	Eto-PLGA-PLU NP			Eto-PLGA-mPEG NP		
	% Labeled	% Colloids	% Free	% Labeled	% Colloids	% Free
25	89.11	8.02	2.85	75.23	1.98	22.79
50	92.43	2.42	5.14	80.12	1.78	18.10
75	96.41	3.12	0.47	90.45	0.89	8.66
100	98.39	0.22	1.34	99.38	0.42	0.20
125	91.10	5.41	3.50	93.15	2.75	4.10
150	90.40	6.10	3.50	95.12	3.45	1.43

Stability studies of the radiolabeled formulations were carried studied in serum for 24 hours, the results obtained are shown in Table 7.3. It was seen that all the five ^{99m}Tc labeled formulations were stable up to 24 hours in serum; ^{99m}Tc- Eto (^{99m}Tc labeled etoposide), ^{99m}Tc- Eto-PLGA NP₁₀₅ (^{99m}Tc labeled etoposide loaded PLGA-NP having MPS of 105nm), ^{99m}Tc- Eto-PLGA NP₁₆₀ (^{99m}Tc labeled etoposide loaded PLGA-NP having MPS of 160nm), ^{99m}Tc- Eto-PLGA-PLU NP (^{99m}Tc labeled etoposide loaded PLGA-Pluronic NP) and ^{99m}Tc- Eto-PLGA-mPEG NP (^{99m}Tc labeled etoposide loaded PLGA-MPEG NP). Stability was indicated by the labeling efficiency of the complex at different time intervals up to 24h. The labeling efficiency was not reduced to less than 97% for any formulations. There was no significant difference (p>0.05) between the labeling efficiency in 15min and at 24 h for all the five labeled formulations. In case of ^{99m}Tc- Etoposide labeling efficiency was 98.12% in 24 hours. 97.32 and 97.12% labeling efficiency was found for ^{99m}Tc- Eto-PLGA NP₁₀₅ and ^{99m}Tc- Eto-PLGA NP₁₆₀ respectively. In case of ^{99m}Tc- Eto-PLGA-PLU NP labeling efficiency in 24h was 97.08 and 98.01% labeling efficiency was found for ^{99m}Tc- Eto-PLGA-mPEG NP. Hence the labeled complexes could be used as biomarkers for biodistribution studies in animals.

Table 7.3
Stability data of ^{99m}Tc- Etoposide, ^{99m}Tc- Eto-PLGA NP and ^{99m}Tc- Eto-PLGA-mPEG NP in serum

Time	% Radiolabeled				
	^{99m} Tc- Eto	^{99m} Tc- Eto- PLGA NP ₁₀₅	^{99m} Tc- Eto- PLGA NP ₁₆₀	^{99m} Tc- Eto- PLGA-PLU NP	^{99m} Tc- Eto- PLGA- mPEG NP
15 min	99.32	99.03	98.32	98.39	99.38
30 min	99.21	99.01	98.13	98.09	99.13
60 min	99.18	98.45	98.03	98.02	98.79
2.0 h	99.15	98.10	97.56	97.85	98.52
4.0 h	99.05	97.75	97.41	97.64	98.13
8.0 h	98.81	97.48	97.40	97.39	98.05
24.0 h	98.12	97.32	97.12	97.08	98.01

The mechanism of labeling of etoposide with ^{99m}Tc was with the two carboxylate groups and one amide group present in the etoposide structure (Reddy et al., 2004). In case of ^{99m}Tc several donor atoms are needed because it can stabilize in different oxidation states, even if one participates in coordination rest will be occupied by oxygen. The amount of stannous chloride used for reduction was optimized based on high labeling efficiency and low colloid formation. Use of more than the optimized amount, stannous chloride leads to formation of colloids and these colloids interfere with the biodistribution studies by distributing themselves to reticuloendothelial system due to their macrophage uptake. Radiocolloid formation was not more than 0.5% for all the five labeled formulations. Use of stannous chloride below the optimum level leads to poor labeling efficiency due to incomplete reduction of pertechnetate from its oxidation state.

Serum stability was important as the labeled formulation would interact with the proteins in the blood in the animal studies and stability of the formulations in serum indicated their stability in biological environment of the animal body and hence will be useful in carrying out the biodistribution studies.

2.6.2 Cytarabine and cytarabine loaded nanoparticles

Cytarabine and cytarabine loaded PLGA Nanoparticles (Cyt-PLGA NP and Cyt-PLGA-MPEG NP) were radiolabeled with ^{99m}Tc by direct labeling procedure using stannous chloride method. Cyt, Cyt-PLGA NP and Cyt-PLGA-MPEG NP were labeled with efficiency more than 98% at pH 6.5. Table 7.4a and 7.4b shows the effect of amount of stannous chloride on the labeling efficiency of Cytarabine and Cytarabine loaded PLGA Nanoparticles. It was seen that 100 $\mu\text{g/ml}$ of stannous chloride was optimum for labeling of Cytarabine having labeling efficiency of 99.19%. In case of Cytarabine loaded PLGA Nanoparticles, 125 μg of stannous chloride was found to be optimum for labeling efficiency of 99.15% and 98.10% for Cyt-PLGA NP and Cyt-PLGA-MPEG NP respectively.

Radiocolloids are formed during the process of labeling and distribute extensively to the organs of RES when injected in animal; therefore they may interfere in the results of the biodistribution studies (Banerjee et al., 2005). Radiocolloid formation during the labeling was less than 1.0% in all the three labeled formulations (Table 7.4a and 7.4b) and hence no interference was expected by them in the biodistribution studies.

Stability of ^{99m}Tc -CYT, ^{99m}Tc -CYT-PLGA NP and ^{99m}Tc -CYT-PLGA-MPEG NP were studied in serum for 24 hours. The results obtained are shown in Table 7.5. It was seen that the labeled complexes were stable up to 24 hours. In case of ^{99m}Tc -CYT, labeling efficiency was 98.18% in 24 hours. In case of ^{99m}Tc -CYT-PLGA NP and ^{99m}Tc -CYT-PLGA-MPEG NP, labeling efficiency was 97.12 and 96.02% respectively. The stability of more than 96% in serum indicated that the radiolabeled formulations could be used in animals for carrying out the biodistribution studies.

Table 7.4a
Effect of amount of stannous chloride on the labeling efficiency of Cytarabine

Stannous Chloride (μg)	Cytarabine		
	% Labeled	% Colloids	% Free
25	87.23	5.02	7.75
50	97.42	1.32	1.26
75	98.43	0.18	1.39
100	99.19	0.12	0.69
125	94.14	4.41	1.45
150	92.58	6.12	1.30

Table 7.4b
Effect of amount of stannous chloride on the labeling efficiency of cytarabine loaded PLGA NPs.

Stannous Chloride (μg)	Cyt-PLGA NP			Cyt-PLGA-MPEG NP		
	% Labeled	% Colloids	% Free	% Labeled	% Colloids	% Free
25	78.23	4.98	16.79	82.32	7.38	10.00
50	87.32	3.78	8.90	89.25	5.43	5.30
75	95.55	2.89	1.56	92.54	4.78	2.70
100	97.28	1.42	1.30	97.10	1.50	1.40
125	99.15	0.55	0.30	98.10	0.49	0.29
150	97.12	2.45	0.43	96.10	2.15	0.59

Table 7.5
Stability data of ^{99m}Tc -CYT, ^{99m}Tc - CYT-PLGA NP in serum

Time	% Radiolabeled		
	^{99m}Tc -CYT	^{99m}Tc - CYT- PLGA NP	^{99m}Tc - CYT- PLGA-MPEG NP
15 min	99.19	99.15	98.10
30 min	99.12	99.08	97.45
60 min	99.08	98.67	97.03
2.0 h	99.05	98.55	96.84
4.0 h	99.01	97.45	96.43
8.0 h	98.13	97.28	96.12
24.0 h	98.18	97.12	96.02

The N,S and O atoms of the reduced ^{99m}Tc species are chemically reactive and act as donor atoms to combine with wide variety of ligands bearing chemical groups such as –COOH, -OH, -NH₂, and –SH. In the cytarabine structure, –OH and -NH₂ groups were thought to be involved in the complex formation with ^{99m}Tc .

SECTION B-BIODISTRIBUTION STUDIES

7.7 Introduction

Surface characteristics and size are the major determinants of the clearance kinetics and biodistribution of colloidal particles. Injected particles would end up in the liver and the spleen macrophages (Juliano, 1988). Approaches taken to avoid the uptake of the injected particles by the reticuloendothelial system (RES) include proper adjustment of particle properties such as size, surface charge, and surface hydrophobicity/ hydrophilicity (Davis et al., 1986).

Covering the colloidal particles with hydrophilic, nonionic polymers greatly increased their stability in the blood circulation due to enhanced stability of such sterically stabilized particles in the blood compartment by their ability to prevent the adsorption of various blood components onto their surface. Steric stabilization confers a relative 'invisibility' to the colloidal particles, which is reflected by a reduced uptake by liver and spleen macrophages and extended blood circulation times (Davis and Illum 1988). Therefore, the use of hydrophilic coatings to decrease uptake of circulating colloidal particles by the RES has become an important recent development.

Regarding the surface coating materials, the block copolymers of ethylene oxide (EO) and propylene oxide (PO), commercially available as poloxamers are the most extensively investigated substances. Poloxamers consist of two EO polymers attached to the ends of one PO polymer. The polymeric surfactants of the poloxamer series have the A-BA block structure; they attach themselves onto the surface of colloidal particles via their central hydrophobic (polyoxypropylene or polyoxypropylene ethylene diamine, respectively) portion (B) while leaving the hydrophilic portion on the surface. The hydrophilic particles remain in the bloodstream for longer periods of time therefore the poloxamers can modify the kinetics of blood clearance of particles. Early observations regarding the utility of poloxamers for RES avoidance were made with poloxamer-188 and -338. (Illum and Davis 1984). Illum and Davis (1983) reported that both poloxamer materials when adsorbed to polystyrene nanoparticles can give rise to a prolonged circulation time and a substantial reduction in liver uptake in rabbits. For the nanoparticles coated with poloxamer- 188, the decrease in hepatosplenic uptake (as compared to uncoated particles) was of the order of 20% at 20 min after administration.

Polyethylene glycol (PEG) polymers are at present the most popular materials for RES avoidance and blood residence prolongation of nanoparticles. They extend the circulation times of particles by diverting them away from the liver and the spleen. Gref et al.(1994) examined the efficacy of covalently attached PEG to alter the biodistribution of nanoparticles composed of poly(lactic-co-glycolic acid) (PLGA). Biodistribution studies performed in mice showed that the blood circulation time of PEGylated particles increased, whereas 66% of the noncoated particles were removed by the liver in less than 15 min.

Biodistribution of the three radiolabeled etoposide loaded PLGA nanoparticles was studied in mice. The first type consisted of conventional uncoated PLGA nanoparticles having two sizes. In this case we studied the influence of mean particle size on the biodistribution of PLGA nanoparticles of sizes 105nm and 160nm (^{99m}Tc -Eto-PLGA NP105 and ^{99m}Tc -Eto-PLGA NP160) and compared it with the biodistribution of pure drug (^{99m}Tc -Eto). The second type of etoposide loaded PLGA nanoparticles were those which were coated with hydrophilic polymer Pluronic F-68 (^{99m}Tc -Eto-PLGA-PLU NP) and finally the third type consisted of Pegylated PLGA NPs of etoposide coated with mPEG (^{99m}Tc -Eto-PLGA-MPEG NP). The physical characteristics of the formulations have been first indicated in the Table 7.1.

In the second section we studied the biodistribution of two types of radiolabeled cytarabine loaded PLGA nanoparticles in mice. The first type consisted of conventional uncoated PLGA nanoparticles (^{99m}Tc -Cyt-PLGA NP). The second type of cytarabine loaded PLGA nanoparticles were of Pegylated PLGA NPs coated with mPEG (^{99m}Tc -Cyt-PLGA-MPEG NP). In both the cases the biodistribution pattern was compared to the biodistribution of pure drug cytarabine. The physical characteristics of the formulations have been indicated in the Table 7.6.

7.8 Biodistribution studies

Balb/c mice having body weight between 20–25 g were used in group of three for these studies. Radiolabeled formulations were injected intravenously (100 µl) in the tail vein of the mice. At time points 1 h, 4h and 24 h after the injection, animals were anaesthetized with chloroform and blood was collected by cardiac puncture in pre-weighed tubes. Mice was then dissected and each organ to be tested (heart, lungs, liver, spleen, kidneys, stomach, intestine, muscle, and brain) was removed. The whole organs were weighed and the radioactivity was counted per gram of the tissue/organ in the gamma ray spectrometer (GRS23C, Electronics Corporation of India Ltd.) The radioactivity remaining in the tail was also measured and taken into consideration in the calculation of total radioactivity dose administered to the mice.

Statistical Analysis

Statistical comparisons of the experimental results were performed by 1-way analysis of variance (ANOVA) at an α level of 0.05. The difference in results between the two groups was compared at the significance levels of $P < 0.05$.

Physicochemical characteristics of the formulations

Table 7.6
Physicochemical characteristics etoposide loaded NPs used in biodistribution studies in mice

Formulation	MPS \pm SD	PdI \pm SD (for MPS)	Zeta potential (mV)	%EE \pm SD
^{99m} Tc-Eto-PLGA NP ₁₀₅	105 \pm 9	0.05 \pm 0.02	-32.2	77.42 \pm 4.2
^{99m} Tc-Eto-PLGA NP ₁₆₀	160 \pm 12	0.08 \pm 0.02	-29.6	83.12 \pm 8.3
^{99m} Tc-Eto-PLGA- PLU NP	148.0 \pm 2.1	0.11 \pm 0.05	-25.1	73.12 \pm 0.7
^{99m} Tc-Eto-PLGA- MPEG NP	94.02 \pm 3.4	0.03 \pm 0.02	-21.2	71.22 \pm 1.1

7.9 Results and discussions for Biodistribution studies

7.9.1 Etoposide and etoposide loaded nanoparticles

7.9.1.1 Biodistribution of ^{99m}Tc -Eto-PLGA NP₁₀₅ and ^{99m}Tc -Eto-PLGA NP₁₆₀

The biodistribution of intravenously injected ^{99m}Tc labeled formulations was performed in Balb/c mice and radioactivity was determined as the percentage injected dose/gram of organ or tissue after 1, 4 and 24h post injection. Table 7.7 shows biodistribution pattern of ^{99m}Tc -Etoposide. Greater concentration of free etoposide was seen in lungs, liver and spleen as compared to blood.

Table 7.7
Biodistribution Studies of ^{99m}Tc -Etoposide in Mice

Organ/Tissue	Percentage Injected Dose/gram of organ/ tissue					
	1h		4h		24 h	
	Mean	SD	Mean	SD	Mean	SD
Blood	1.25	0.08	1.02	0.03	0.38	0.08
Heart	0.42	0.04	0.30	0.002	0.25	0.025
Lungs	15.04	1.80	14.00	2.60	12.67	1.30
Liver	4.00	0.23	3.40	0.50	2.64	0.50
Spleen	13.20	2.60	11.10	1.70	9.69	1.70
Kidney	3.55	0.06	3.30	0.20	1.00	0.20
Stomach	0.30	0.10	0.50	0.10	0.32	0.10
Intestine	1.20	0.40	0.80	0.20	0.68	0.12
Muscle	0.40	0.07	0.50	0.40	0.46	0.12
Brain	0.06	0.02	0.04	0.01	0.02	0.01
Bone	0.21	0.03	0.09	0.02	0.08	0.02

^{99m}Tc indicates Technetium-99m. Each value is the mean (\pm SD) of 3 mice

The biodistribution pattern of conventional etoposide loaded PLGA nanoparticles, ^{99m}Tc - Eto-PLGA NP₁₀₅ and ^{99m}Tc - Eto-PLGA NP₁₆₀ is shown in Table 7.8. There was a different biodistribution pattern seen in the two etoposide loaded PLGA NPs, which was probably due to the difference in their mean particle sizes. There was a significant difference ($p < 0.05$) in the three formulations, ^{99m}Tc - Eto, ^{99m}Tc - Eto-PLGA NP₁₀₅ and ^{99m}Tc - Eto-PLGA NP₁₆₀, in terms of percentage of injected dose found in the blood in 1h, 4h and 24h.

Table 7.8
Biodistribution Studies of ^{99m}Tc-Eto-PLGA NP₁₀₅ and ^{99m}Tc-Eto-PLGA NP₁₆₀ in Balb/c Mice

Organ/ Tissue	Percentage Injected Dose/gram of organ/ tissue											
	^{99m} Tc-Eto-PLGA NP ₁₀₅						^{99m} Tc-Eto-PLGA NP ₁₆₀					
	1h		4h		24h		1h		4h		24h	
	Mean	SD	Mean	SD	Mean	SD	Mean	SD	Mean	SD	Mean	SD
Blood	5.80	0.08	4.02	0.10	3.98	0.08	3.10	0.09	2.06	0.10	1.08	0.08
Heart	0.52	0.04	0.40	0.007	0.35	0.03	0.41	0.04	0.30	0.005	0.15	0.02
Lungs	5.14	1.10	3.60	0.60	2.07	0.08	8.94	1.50	7.50	1.01	9.17	1.02
Liver	1.40	0.13	1.00	0.03	0.84	0.08	4.30	0.12	6.30	0.03	2.94	0.80
Spleen	4.20	0.50	5.80	0.70	3.00	0.60	13.20	2.10	15.10	1.70	9.60	1.70
Kidney	2.15	0.06	2.30	0.20	0.80	0.20	1.85	0.06	2.20	0.20	0.70	0.20
Stomach	0.35	0.10	0.53	0.10	0.38	0.10	0.30	0.10	0.40	0.10	0.31	0.10
Intestine	1.06	0.10	0.70	0.20	0.58	0.12	1.02	0.10	0.50	0.20	0.41	0.12
Muscle	0.20	0.07	0.10	0.40	0.06	0.12	0.18	0.06	0.11	0.30	0.04	0.02
Brain	0.58	0.08	0.60	0.02	0.22	0.01	0.07	0.02	0.03	0.01	0.02	0.01
Bone	0.31	0.03	0.49	0.02	0.58	0.02	0.21	0.03	0.32	0.02	0.18	0.02

^{99m}Tc indicates Technetium-99m. ^{99m}Tc-Eto-PLGA NP₁₀₅ and ^{99m}Tc-Eto-PLGA NP₁₆₀ indicates Technetium-99m labeled etoposide loaded PLGA NPs having mean particle size of 105nm, and ^{99m}160nm respectively. Each value is the mean (\pm SD) of 3 mice.

In the plain drug 1.25% of the injected dose (ID) was found in the blood, whereas in the ^{99m}Tc -Eto-PLGA NP₁₆₀ it was increased to 3.10% and in the formulation it was further increased to 5.85. The increase in the concentration is probably due to the delivery system. Both the NP formulations have MPS less than 200nm, but ^{99m}Tc -Eto-PLGA NP₁₀₅ is much closer to ~100nm, which suggests its greater concentration in the blood. ^{99m}Tc -Eto-PLGA NP₁₀₅ was also able to keep the concentration still high compared to pure drug and ^{99m}Tc -Eto-PLGA NP₁₆₀ up to 24h. The visual representation of the comparative distribution of the three formulations is shown in the figure 7.1. In 24h pure drug concentration was reduced to 0.38% and ^{99m}Tc -Eto-PLGA NP₁₆₀ was reduced to 1.08%, where as ^{99m}Tc -Eto-PLGA NP₁₀₅ was still holding a high comparative concentration of 3.98%, which was about ten times more than the pure drug and about 3.6 fold more than ^{99m}Tc -Eto-PLGA NP₁₆₀. This suggested that ^{99m}Tc -Eto-PLGA NP₁₀₅ could remain the blood circulation for a longer duration and higher concentration.

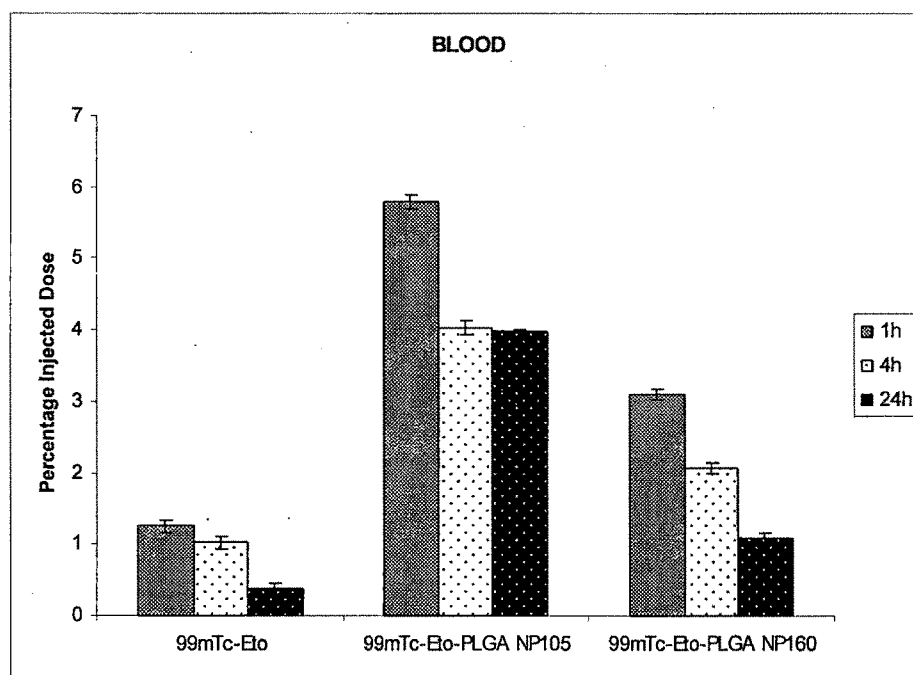


Fig. 7.1: Concentrations of ^{99m}Tc -Eto, ^{99m}Tc -Eto-PLGA NP₁₀₅ and ^{99m}Tc -Eto-PLGA NP₁₆₀ in the blood of Balb/c mice at 1h, 4h and 24h interval post injection. Each value is the mean (\pm SD) of 3 mice

The biodistribution of these formulations in the liver and spleen organs, which are the major organs of the RES system, is shown in Fig. 7.2. It was interesting to note that the biodistribution pattern of ^{99m}Tc -Eto-PLGA NP₁₆₀ was similar to that of ^{99m}Tc -Eto in liver in the first hour and at 24h and there was no significant difference ($p < 0.05$) found in the concentration of the two. Whereas the concentration of ^{99m}Tc -Eto-PLGA NP₁₆₀ at 4h was higher than ^{99m}Tc -Eto. Similarly the biodistribution pattern of ^{99m}Tc -Eto-PLGA NP₁₆₀ was similar to that of ^{99m}Tc -Eto in spleen in the first hour and at 24h and there was no significant difference ($p < 0.05$) found in the concentration of the two. Whereas the concentration of ^{99m}Tc -Eto-PLGA NP₁₆₀ at 4h was higher than ^{99m}Tc -Eto. This suggests that the larger nanoparticles of PLGA have nearly the same or even more affinity towards the liver and spleen than the NPs of size close to ~100nm. There was a significant difference in the concentration of ^{99m}Tc -Eto-PLGA NP₁₀₅ in both the liver and spleen ($p > 0.05$), compared to ^{99m}Tc -Eto and ^{99m}Tc -Eto-PLGA NP₁₆₀

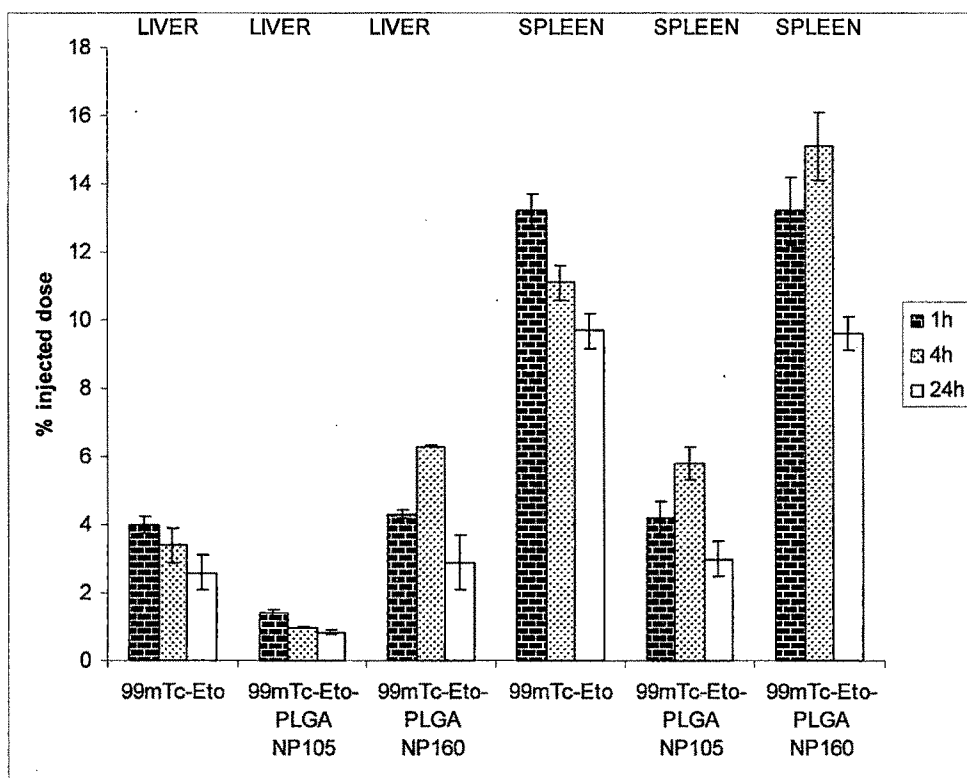


Fig. 7.2: Concentrations of ^{99m}Tc -Eto, ^{99m}Tc -Eto-PLGA NP₁₀₅ and ^{99m}Tc -Eto-PLGA NP₁₆₀ in the Liver and Spleen of Balb/c mice at 1h, 4h and 24h interval post injection. Each value is the mean (\pm SD) of 3 mice

The concentration of ^{99m}Tc -Eto-PLGA NP₁₀₅ was only 0.8% of the ID, which was about 3.3 times and 3.6 times less than the concentration of ^{99m}Tc -Eto and ^{99m}Tc -Eto-PLGA NP₁₆₀ respectively in the liver in 24h. Similarly in spleen, in 24h, the concentration of ^{99m}Tc -Eto-PLGA NP₁₀₅ was 3.0% of the ID, which was about 3.2 times less than the concentration of both ^{99m}Tc -Eto and ^{99m}Tc -Eto-PLGA NP₁₆₀. The results indicate that ^{99m}Tc -Eto-PLGA NP₁₀₅ have a much lower affinity towards liver and spleen and therefore would remain in the blood circulation for a much longer duration.

The biodistribution of free drug ^{99m}Tc -Eto in lungs was much higher than the two nanoparticulate formulations (Fig. 7.3). And among the two NPs, ^{99m}Tc -Eto-PLGA NP₁₀₅ had much lower concentration than ^{99m}Tc -Eto-PLGA NP₁₆₀. There was a much greater significant difference ($p > 0.05$) in the concentration of biodistribution of the three labeled formulations in the lungs of the mice. In 24h, the concentration of ^{99m}Tc -Eto-PLGA NP₁₀₅ was about 2.0% of the ID, which was about 6 times less than the concentration of ^{99m}Tc -Eto and about 4.4 times less than the concentration of ^{99m}Tc -Eto-PLGA NP₁₆₀.

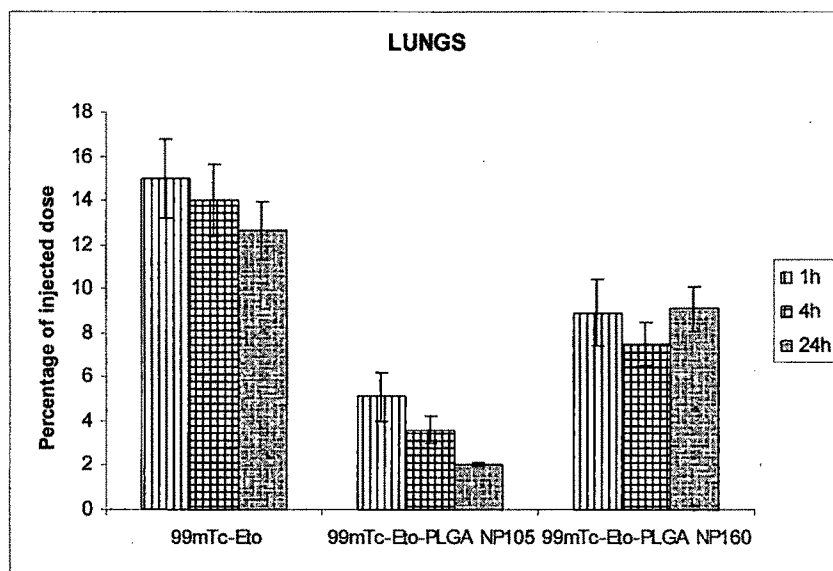


Fig. 7.3: Concentrations of ^{99m}Tc -Eto, ^{99m}Tc -Eto-PLGA NP₁₀₅ and ^{99m}Tc -Eto-PLGA NP₁₆₀ in the lungs of Balb/c mice at 1h, 4h and 24h interval post injection. Each value is the mean (\pm SD) of 3 mice

The pure drug ($^{99m}\text{Tc-Eto}$) did not cross BBB and therefore had negligible presence in the brain. The biodistribution pattern in the brain had a very significant difference in the uptake of the two NP, $^{99m}\text{Tc-Eto-PLGA NP}_{105}$ and $^{99m}\text{Tc-Eto-PLGA NP}_{160}$ (Fig. 7.4). $^{99m}\text{Tc-Eto-PLGA NP}_{105}$ showed relatively high concentrations of 0.58% of ID in brain in 1h (8 folds higher), 0.6% in 4h (20 folds higher) and 0.22% in 24h (10 folds higher) than the concentration of $^{99m}\text{Tc-Eto-PLGA NP}_{160}$. Oliver (2005) had suggested that particles with diameter $\sim 100\text{nm}$ could cross the BBB. Hence the difference in the brain uptake of the two NPs might be attributed to the difference in their mean particle sizes.

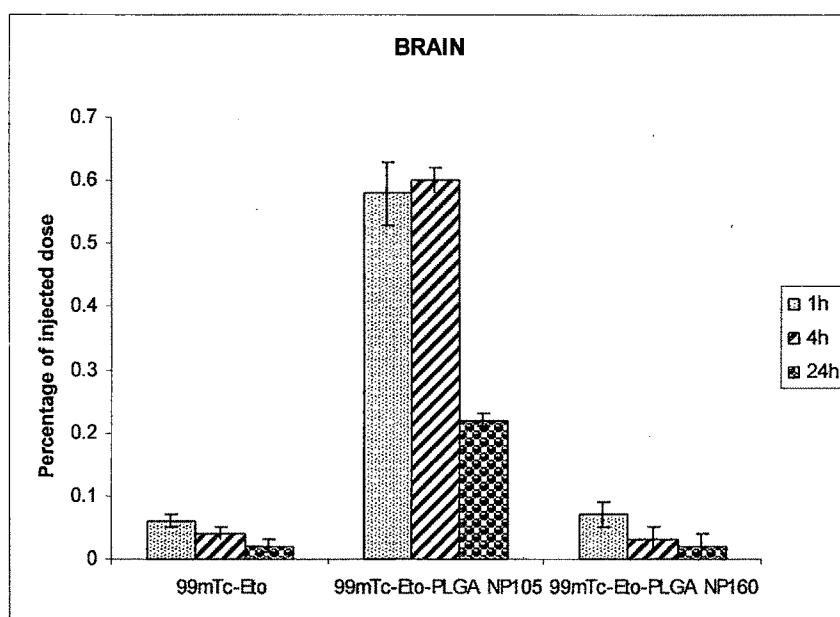


Fig. 7.4: Brain concentrations of $^{99m}\text{Tc-Eto}$, $^{99m}\text{Tc-Eto-PLGA NP}_{105}$ and $^{99m}\text{Tc-Eto-PLGA NP}_{160}$ in Balb/c mice at 1h, 4h and 24h interval post injection. Each value is the mean (\pm SD) of 3 mice

The biodistribution in femur bone of the mice had significant different results in the three formulations (Fig. 7.5). There was no significant difference in the concentration of $^{99m}\text{Tc-Eto}$ and $^{99m}\text{Tc-Eto-PLGA NP}_{160}$ in brain the first hour. However, as the time increased, the concentration of $^{99m}\text{Tc-Eto}$ decreased to 0.08% of the ID in 24h. The concentration of $^{99m}\text{Tc-Eto-PLGA NP}_{160}$ increased from 0.21 to 0.32% of the ID in 4h, but then reduced to 0.18% of the ID. But even this concentration of $^{99m}\text{Tc-Eto-PLGA NP}_{160}$ was about 2.2 times higher than the concentration of $^{99m}\text{Tc-Eto}$ in 24h.

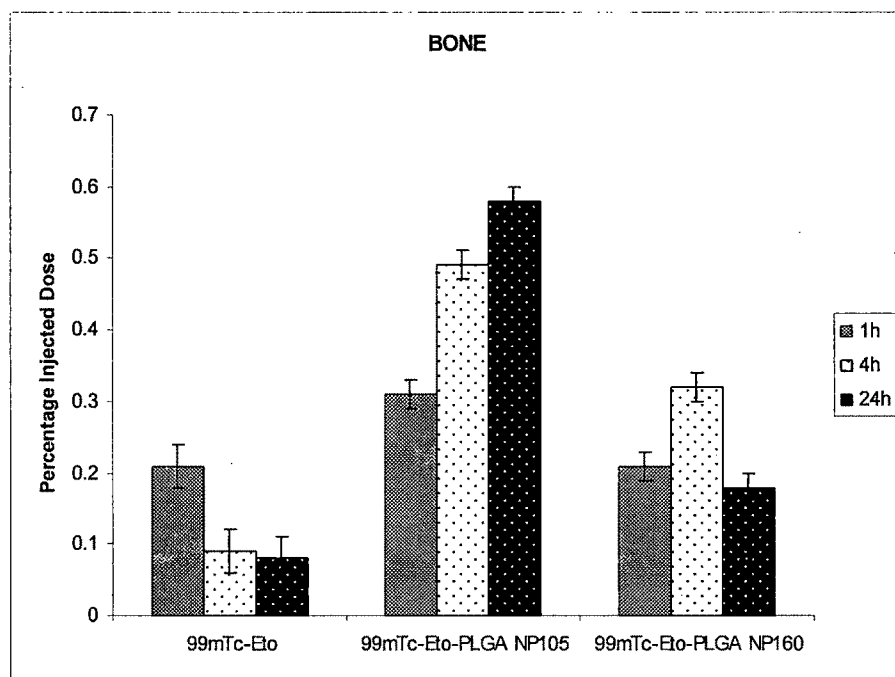


Fig. 7.5: Bone concentrations of $^{99m}\text{Tc-Eto}$, $^{99m}\text{Tc-Eto-PLGA NP}_{105}$ and $^{99m}\text{Tc-Eto-PLGA NP}_{160}$ in Balb/c mice at 1h, 4h and 24h interval post injection. Each value is the mean (\pm SD) of 3 mice

No significant difference in the uptake of the three formulations was seen in the intestine, stomach and muscle.

Conclusion

From the results of the radiolabeled ETO and radiolabeled ETO loaded PLGA NPs of two sizes, 105 and 160nm, it was concluded that PLGA NP of size 105 ($^{99m}\text{Tc-Eto-PLGA NP}_{105}$) were present at a higher concentration in the circulation and at lower concentration in liver, spleen and lungs as compared to $^{99m}\text{Tc-Eto}$ (Pure drug ETO) and $^{99m}\text{Tc-Eto-PLGA NP}_{160}$ (PLGA NP of size 160nm). This was probably due to the fact that nanoparticles of size less than 100 nm diameter can evade the RES and have a long circulation time in the blood (Gaur et al., 2000). In the present study, it was concluded that PLGA-NP of size \sim 100nm were present in the blood at higher concentrations upto 24h and were able to reduce their uptake by the RES as compared to the pure drug.

7.9.1.2 Biodistribution Studies of ^{99m}Tc -Eto-PLGA-PLU NP and ^{99m}Tc -Eto-PLGA-mPEG NP

The Biodistribution Studies of ^{99m}Tc -Eto-PLGA-PLU NP and ^{99m}Tc -Eto-PLGA-mPEG NP (Technetium-99m labeled etoposide loaded PLGA-Pluronic NPs and Technetium-99m labeled etoposide loaded pegylated PLGA-MPEG NP) in Balb/c Mice is shown in Table 7.9. It was seen that the biodistribution of the two surface modified PLGA based NPs was significantly different than that of the free drug. The concentration of the two formulations in blood was the highest as compared to other organs/tissues. The concentrations of the two NP formulations were also higher in the blood compared to free drug. A graph was plotted to have a visual representation of their uptake in blood and compare it to free drug (Fig.7.6). The biodistribution pattern of the two surface modified NP formulations was similar but they were significantly different ($p > 0.05$) from each other. The concentration of ^{99m}Tc -Eto-PLGA-PLU NP and ^{99m}Tc -Eto-PLGA-mPEG NP was 10.15% and 11.25% respectively of the ID in 1h, whereas the concentration of pure drug was only 1.25% of the ID in 1h. This means that there was an increase in the uptake of the ^{99m}Tc -Eto-PLGA-PLU NP by 8.12 times and ^{99m}Tc -Eto-PLGA-mPEG NP by 9.0 times in blood in 1h. After 4h, the uptake of both the NP formulations was increased and it was 8.8 times for ^{99m}Tc -Eto-PLGA-PLU NP and 9.8 times for ^{99m}Tc -Eto-PLGA-MPEG NP. There was a drastic increase in concentration at 24h for ^{99m}Tc -Eto-PLGA-PLU NP as compared to the free drug, which was about 21.8 folds greater. Similarly, there was increase in the uptake of ^{99m}Tc -Eto-PLGA-MPEG NP in 24h by 26.2 times than that of the free drug.

The results of the biodistribution studies of the two surface modified etoposide loaded NP, ^{99m}Tc -Eto-PLGA-PLU NP and ^{99m}Tc -Eto-PLGA-mPEG NP show that they were present in the blood circulation at much higher concentrations upto 24h than that of the free drug, which was negligible after 4h.

Table 7.9
Biodistribution Studies of ^{99m}Tc- Eto-PLGA-PLU NP and ^{99m}Tc- Eto-PLGA-mPEG NP in Balb/c Mice

Organ/ Tissue	Percentage Injected Dose/gram of organ/ tissue											
	^{99m} Tc-Eto-PLGA-PLU NP						^{99m} Tc-Eto-PLGA-mPEG NP					
	1h		4h		24h		1h		4h		24h	
	Mean	SD	Mean	SD	Mean	SD	Mean	SD	Mean	SD	Mean	SD
Blood	10.15	1.18	9.02	0.08	8.38	0.09	11.25	1.08	10.02	0.07	9.98	0.08
Heart	0.61	0.08	0.53	0.07	0.41	0.05	0.72	0.08	0.63	0.07	0.55	0.05
Lungs	5.02	1.12	6.10	1.05	3.07	0.42	6.04	1.02	5.20	1.01	3.17	0.48
Liver	1.89	0.03	1.51	0.03	1.06	0.02	1.20	0.03	1.10	0.03	0.86	0.02
Spleen	2.30	0.30	2.10	0.80	1.09	0.60	1.80	0.40	1.10	0.20	0.20	0.02
Kidney	1.60	0.06	1.10	0.20	1.03	0.02	1.50	0.06	1.30	0.20	1.00	0.02
Stomach	0.43	0.10	0.32	0.10	0.21	0.10	0.33	0.10	0.40	0.10	0.22	0.10
Intestine	1.06	0.10	0.50	0.22	0.38	0.20	1.02	0.30	0.70	0.20	0.58	0.2
Muscle	0.13	0.07	0.08	0.02	0.03	0.02	0.10	0.07	0.05	0.02	0.02	0.02
Brain	3.21	0.09	2.14	0.07	2.82	0.06	2.01	0.05	2.24	0.07	1.12	0.05
Bone	0.81	0.04	1.09	0.02	0.94	0.03	0.61	0.03	0.49	0.02	0.58	0.02

^{99m}Tc indicates Technetium-99m. ^{99m}Tc- Eto-PLGA-PLU NP and ^{99m}Tc- Eto-PLGA-mPEG NP indicates Technetium-99m labeled etoposide loaded PLGA-Pluronic NPs and PLGA-mPEG NPs respectively. Each value is the mean (\pm SD) of 3 mice.

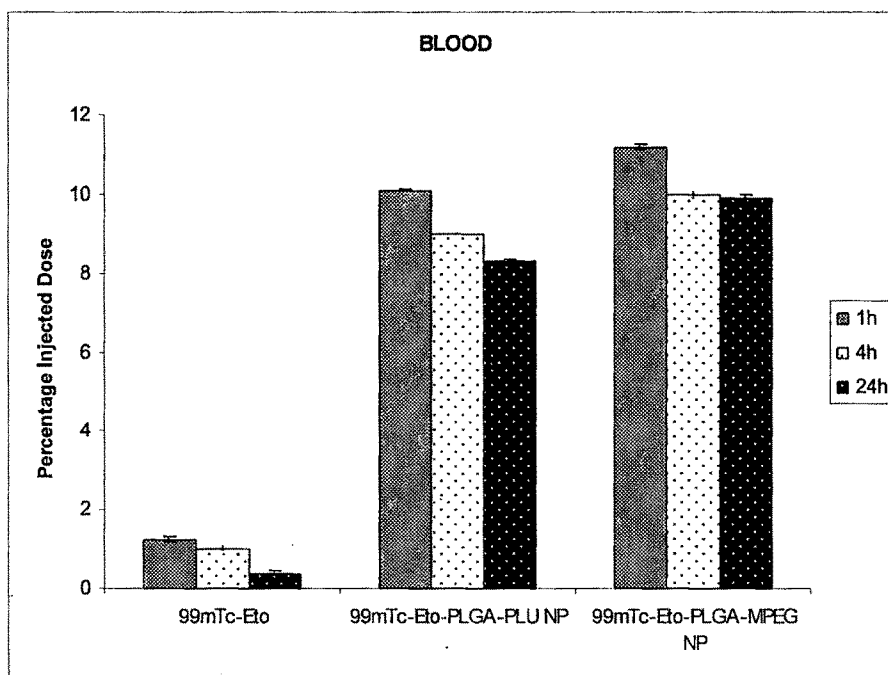


Fig.7.6: Blood concentrations of ^{99m}Tc-Eto-PLGA-PLU NP and ^{99m}Tc-Eto-PLGA-mPEG NP in Balb/c mice at 1h, 4h and 24h interval post injection. Each value is the mean (\pm SD) of 3 mice

The uptake profile in the RES organs- liver, spleen and lungs is shown in Fig.7.7. There was a significant difference in the uptake of NPs by spleen than liver compared to free drug. In the liver, the uptake of ^{99m}Tc-Eto-PLGA-PLU NP was reduced by 2.1 times and the uptake of ^{99m}Tc-Eto-PLGA-mPEG NP was reduced by 3.3 times compared to the free drug (^{99m}Tc-Eto) in the first hour. The uptake of ^{99m}Tc-Eto-PLGA-PLU NP and ^{99m}Tc-Eto-PLGA-mPEG NP was further reduced by 2.2 times and 3.0 times in the 4h as compared to ^{99m}Tc-Eto in liver. The uptake in the 24h was further reduced by 2.4 times and 3.2 times for ^{99m}Tc-Eto-PLGA-PLU NP and ^{99m}Tc-Eto-PLGA-mPEG NP respectively by liver.

The uptake of NPs by spleen was reduced by much higher concentrations as compared to pure drug. In the spleen, the uptake of ^{99m}Tc-Eto-PLGA-PLU NP was reduced by 5.7 times and uptake of ^{99m}Tc-Eto-PLGA-mPEG NP was reduced by 7.3 times than that of the free drug (^{99m}Tc-Eto) in the first hour. In the 4h, the uptake was further reduced by 5.2 times for ^{99m}Tc-Eto-PLGA-PLU NP and 10.0 times for ^{99m}Tc-Eto-PLGA-mPEG NP. Highest reduction of uptake was seen in 24h. Uptake of ^{99m}Tc-

Eto-PLGA-PLU NP was reduced by 8.8 times and uptake of ^{99m}Tc -Eto-PLGA-mPEG NP was reduced by 48.4 times (only 0.20% of ID) by spleen in 24h compared to free drug (^{99m}Tc -Eto) which was 9.6% of the ID.

Similar reduction in the uptake of the NPs was observed for the next RES organ, lungs. There was a reduction of uptake by 3 times (5.02%) for ^{99m}Tc -Eto-PLGA-PLU NP in lungs and a reduction of 2.5 times (6.0% of ID) for ^{99m}Tc -Eto-PLGA-mPEG NP as compared to pure drug. In 24h the reduction was further increased by 4.2 times for ^{99m}Tc -Eto-PLGA-PLU NP and by 4.0 times by ^{99m}Tc -Eto-PLGA-mPEG NP as compared to free drug (^{99m}Tc -Eto) in lungs.

The results clearly indicate that the uptake of the two surface modified NPs by the RES organs (liver, spleen and lungs) was drastically reduced. It has been reported that PEGylated nanoparticles (Gref et al., 1994) and nanoparticles coated with Poloxamers (Illum et al., 1987) significantly reduce their liver and spleen uptake due to their surface hydrophilicity.

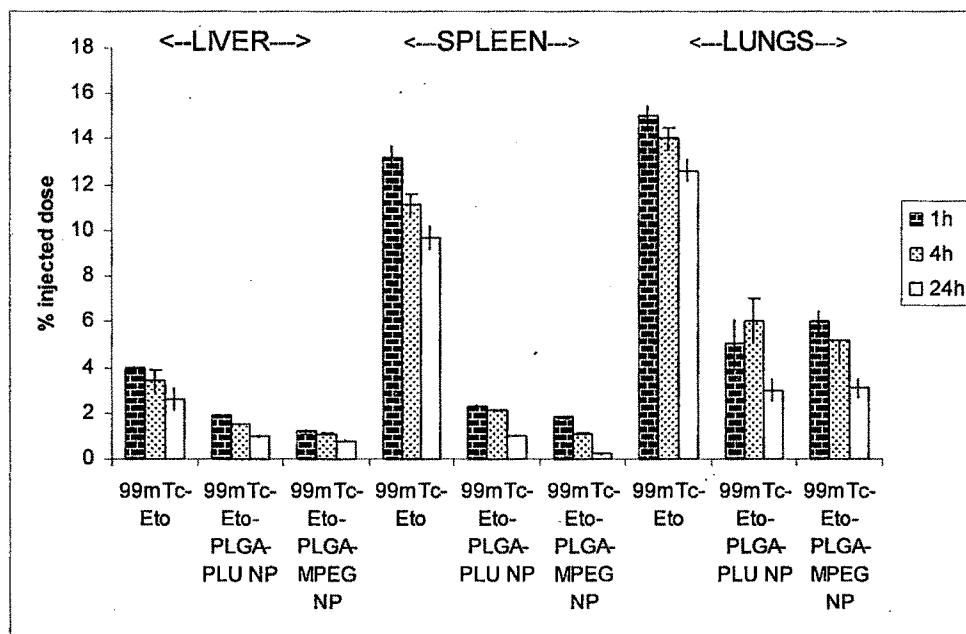


Fig. 7.7: Liver, Spleen and Lungs concentrations of ^{99m}Tc -Eto-PLGA-PLU NP and ^{99m}Tc -Eto-PLGA-mPEG NP in Balb/c mice at 1h, 4h and 24h interval post injection. Each value is the mean (\pm SD) of 3 mice

The other organs which showed significant difference in the uptake were brain and bones. There was a drastic increase in the biodistribution concentration of the NPs in the mice brain as compared to free drug etoposide. There was a significant difference in the uptake of ^{99m}Tc -Eto-PLGA-PLU NP and ^{99m}Tc -Eto-PLGA-MPEG NP compared to ^{99m}Tc -Eto (Fig. 7.8). ^{99m}Tc -Eto-PLGA-PLU NP showed relatively higher concentrations than ^{99m}Tc -Eto-PLGA-MPEG NP in brain. In 1h, ^{99m}Tc -Eto-PLGA-PLU NP had brain concentration of 3.2% ID, whereas ^{99m}Tc -Eto had only 0.06% ID. This indicates 53 times greater concentration than the pure drug. In the 4h also the uptake was around 50 times higher, but in the 24h the uptake was highest and it was 140 times more than the pure drug (2.82% for ^{99m}Tc -Eto-PLGA-PLU NP and only 0.02% for ^{99m}Tc -Eto) in 24h. Uptake of ^{99m}Tc -Eto-PLGA-MPEG NP was also high, but not as high as that of ^{99m}Tc -Eto-PLGA-PLU NP. In the first hour, the uptake of ^{99m}Tc -Eto-PLGA-MPEG NP was increased by 33.3 times and in the 24h the uptake was increased by 56 times compared to free drug ^{99m}Tc -Eto in brain.

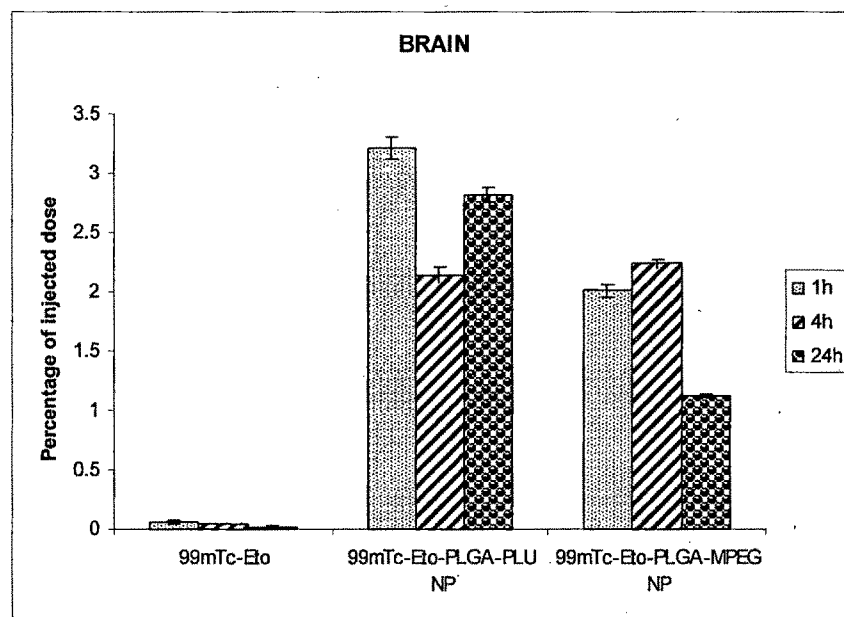


Fig. 7.8: Brain concentrations of ^{99m}Tc -Eto-PLGA-PLU NP and ^{99m}Tc -Eto-PLGA-mPEG NP in Balb/c mice at 1h, 4h and 24h interval post injection. Each value is the mean (\pm SD) of 3 mice.

There was an increase in the uptake of ^{99m}Tc -Eto-PLGA-PLU NP by 3.8 times (0.81% of ID), 11.1 times (1.09% of ID) and 11.7 times (0.94% of ID) in 1, 4 and 24h in bones respectively compared to free drug ^{99m}Tc -Eto (Fig. 7.9). Similarly, there was an increase in the uptake of ^{99m}Tc -Eto-PLGA-MPEG NP in bone but it was less than that of ^{99m}Tc -Eto-PLGA-PLU NP. There was an increase in the uptake of ^{99m}Tc -Eto-PLGA-MPEG NP by 2.9 times (0.61% of ID), 5.4 times (0.49% of ID) and 7.2 times (0.58% of ID) in 1, 4 and 24h respectively compared to free drug ^{99m}Tc -Eto in Femur bone of the mice.

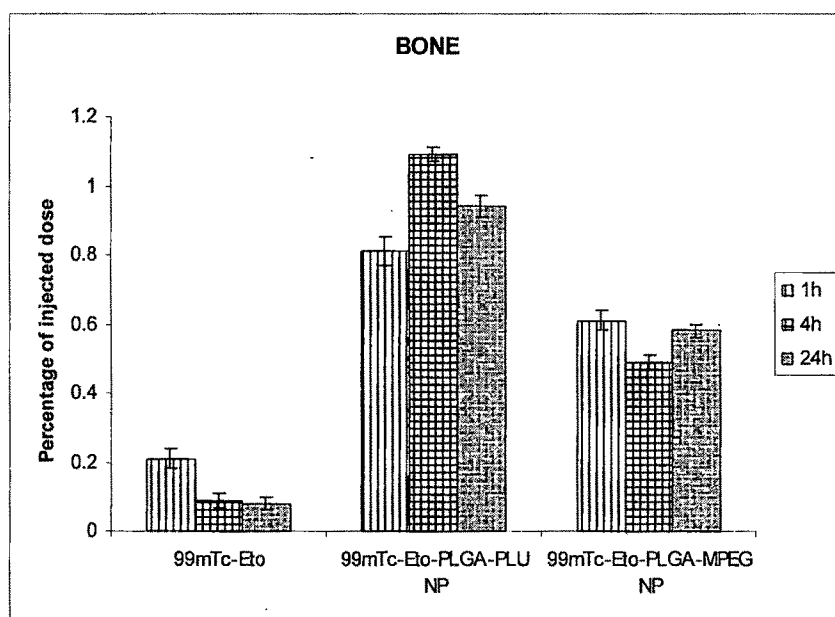


Fig. 7.9: Bone concentrations of ^{99m}Tc -Eto-PLGA-PLU NP and ^{99m}Tc -Eto-PLGA-mPEG NP in Balb/c mice at 1h, 4h and 24h interval post injection. Each value is the mean (\pm SD) of 3 mice

No significant difference in the uptake of the two formulations was seen in the heart, kidney, stomach, intestine, and muscle as compared to the free drug.

Conclusion

The fate of the nanoparticles after IV administration is mainly dependent on the surface hydrophilicity. In the present study, the two NPs surface modified with MPEG and PLU (^{99m}Tc -Eto-PLGA-mPEG NP and ^{99m}Tc -Eto-PLGA-PLU NP) were able to reduce their RES uptake and increase blood concentrations. However, there was a difference in the two probably due to their different surface characteristics.

Decrease in RES uptake of PEG coated particles is possibly due to the presence of steric barrier which decreases the adsorption of plasma proteins on the surface of these nanoparticles. Steric stabilization makes the particle relatively invisible to the macrophages and a reduced uptake by liver and spleen is observed with extended blood circulation times (Moghimi and Davis, 1994)

Pluronic contain polyethylene oxide (PEO) (hydrophilic) and polypropylene oxide (hydrophobic) (PPO) moieties. They are adsorbed to particle surfaces from the hydrophobic moiety (the anchor block) and the hydrophilic block(s) extend on the surface of the particle to form a hydrophilic layer (Redhead et al., 2001). The hydrophilic layer on the surface makes the NP long circulating in the blood and avoids their RES uptake.

Comparing the biodistribution of the two NPs in blood, it was seen that the MPEG modified NP was present in higher concentrations than PLU modified NP at all the time points. Spenlehauer et al. (1994) reported that the biodistribution of PLA NP was modified by use of PEG and Poloxamer 188. They also reported that 50% of the ID was seen in PLA-PEG NP after 5h, whereas Poloxamer coated PLA NP was rapidly cleared from the circulation within 30 min.

7.9.2 Cytarabine and Cytarabine loaded nanoparticles

Table 7.10 shows the physiochemical characteristics of the cytarabine loaded nanoparticles used in biodistribution studies in mice. ^{99m}Tc -Cyt-PLGA NP had a mean particle size of 125nm and ^{99m}Tc -Cyt-PLGA-MPEG NP had a mean particle size of 152nm. The biodistribution of intravenously injected ^{99m}Tc labeled formulations- pure cytarabine (^{99m}Tc -Cyt), cytarabine loaded PLGA NPs (^{99m}Tc -Cyt-PLGA NP) and cytarabine loaded pegylated PLGA NPs (^{99m}Tc -Cyt-PLGA-MPEG NP) was performed in Balb/c mice and radioactivity was determined as the percentage injected dose/gram of organ or tissue after 1, 4 and 24h post injection.

Table 7.10
Physiochemical characteristics of the formulations used in biodistribution studies in mice

Formulation	MPS \pm SD*	PdI \pm SD (for MPS)	Zeta potential \pm SD* (mV)	%EE \pm SD*
^{99m}Tc -Cyt-PLGA NP	125 \pm 12.08 nm	0.25 \pm 0.04	-29.7 \pm 2.18	21.02 \pm 2.91
^{99m}Tc -Cyt-PLGA-MPEG NP	152 \pm 6.48 nm	0.41 \pm 0.06	-23.2 \pm 2.60	33.12 \pm 2.1

* Values indicate mean of three batches. PdI is polydispersity index for the mean particle size. Zeta potential values are at pH 7.4.

Table 7.11 shows biodistribution pattern of ^{99m}Tc -cytarabine. Greater concentration of free etoposide was seen in lungs, liver and spleen, which are organs of the RES than in the blood. The biodistribution pattern of conventional cytarabine loaded PLGA nanoparticles, ^{99m}Tc -Cyt-PLGA NP and pegylated PLGA, ^{99m}Tc -Cyt-PLGA-MPEG NP is shown in Table 7.13. There was a different biodistribution pattern seen in the two etoposide loaded PLGA NPs, which was probably due to the difference in their mean particle sizes. There was a significant difference ($p < 0.05$) in the three formulations, ^{99m}Tc - Eto, ^{99m}Tc - Eto-PLGA NP₁₀₅ and ^{99m}Tc - Eto-PLGA NP₁₆₀, in terms of percentage of injected dose found in the blood in 1h, 4h and 24h.

Table 7.11
Biodistribution Studies of ^{99m}Tc- Cytarabine in Balb/c Mice

organ/ tissue	Percentage Injected Dose/gram of organ/ tissue					
	1h		4h		24 h	
	Mean	SD	Mean	SD	Mean	SD
Blood	1.30	0.08	1.20	0.10	0.20	0.08
Heart	0.60	0.03	0.80	0.007	1.10	0.06
Lungs	4.68	0.50	3.23	1.60	3.30	0.30
Liver	13.37	4.13	23.21	5.03	4.43	1.08
Spleen	15.53	3.60	13.23	3.70	3.53	1.03
Kidney	1.81	0.06	0.21	0.20	0.54	0.12
Stomach	0.91	0.10	0.81	0.10	0.72	0.10
Intestine	0.28	0.10	0.16	0.20	0.05	0.02
Muscle	0.52	0.07	0.62	0.40	0.72	0.12
Brain	0.04	0.01	0.05	0.01	0.07	0.01
Bone	0.08	0.03	0.09	0.02	0.12	0.02

^{99m}Tc indicates Technetium-99m. Each value is the mean (\pm SD) of % injected dose in 3 mice

It was seen that the biodistribution of the two PLGA based NPs is significantly different than that of the free drug. Cyt-PLGA NP is conventional uncoated NP, whereas Cyt-PLGA-MPEG NP is pegylated PLGA NP. The fate of the nanoparticles after IV administration is mainly dependent on the surface hydrophilicity and its size, and hence a significant difference ($p > 0.05$) was also seen in the biodistribution of the two NPs in blood. Firstly as seen in the Table 7.12, the concentration of the ^{99m}Tc-Cyt-PLGA-MPEG NP in blood was the highest as compared to other organs/tissues, whereas the concentration of the ^{99m}Tc-Cyt-PLGA NP was highest in liver. The concentrations of ^{99m}Tc-Cyt-PLGA NP in blood were still higher than the free drug. A graph was plotted to have a visual representation of their uptake in blood and compare it to free drug and shown in Fig. 7.10.

Table 7.12
Biodistribution Studies of ^{99m}Tc-Cyt-PLGA NP and ^{99m}Tc-Cyt-PLGA-MPEG NP in Balb/c Mice

Organ/ Tissue	Percentage Injected Dose/gram of organ/ tissue											
	^{99m} Tc-Cyt-PLGA NP						^{99m} Tc-Cyt-PLGA-MPEG NP					
	1h		4h		24h		1h		4h		24h	
	Mean	SD	Mean	SD	Mean	SD	Mean	SD	Mean	SD	Mean	SD
Blood	2.30	0.08	1.20	0.10	0.40	0.08	20.75	1.18	20.02	1.07	18.21	1.08
Heart	0.62	0.03	0.70	0.007	0.98	0.06	0.53	0.08	0.43	0.07	0.35	0.05
Lungs	3.21	0.02	2.20	0.05	1.67	0.40	1.21	0.02	0.80	0.05	0.60	0.20
Liver	4.21	0.63	3.10	0.63	2.86	1.02	1.24	0.33	2.02	0.13	0.71	0.04
Spleen	3.82	0.60	3.10	0.70	3.00	0.02	1.02	0.30	2.08	0.04	1.23	0.02
Kidney	0.61	0.08	0.42	0.20	0.91	0.04	0.21	0.06	0.30	0.20	1.00	0.02
Stomach	0.82	0.12	0.73	0.15	0.56	0.09	0.52	0.10	0.40	0.10	0.22	0.10
Intestine	0.18	0.07	0.16	0.06	0.15	0.02	0.13	0.30	0.70	0.20	0.58	0.2
Muscle	0.50	0.06	0.68	0.41	0.08	0.02	0.48	0.07	0.09	0.02	0.02	0.02
Brain	0.05	0.01	0.05	0.01	0.07	0.01	0.12	0.05	1.24	0.07	1.62	0.05
Bone	0.21	0.03	0.15	0.02	0.08	0.02	0.18	0.03	0.49	0.02	0.52	0.02

^{99m}Tc indicates Technetium-99m. Each value is the mean (\pm SD) of % injected dose in 3 mice

The concentration of ^{99m}Tc -Cyt-PLGA NP was 2.3% in 1h and ^{99m}Tc -Cyt-PLGA-mPEG NP was 20.75% of the ID, whereas the pure drug was only 1.30%. This means that there was an increase in the uptake of the ^{99m}Tc -Cyt-PLGA NP by 1.7 times and ^{99m}Tc -Eto-PLGA-mPEG NP by 15.9 times in blood in 1h. After 4h the uptake of ^{99m}Tc -Cyt-PLGA NP was same as that of pure drug (^{99m}Tc -Cyt) and even same in the 14h, that means after 4h the concentrations of ^{99m}Tc -Cyt-PLGA NP and pure drug were same in blood. There was a drastic increase in the blood concentrations of ^{99m}Tc -Cyt-PLGA-MPEG NP even in the 4h and 24h, indicating its long circulating behavior. The concentration of ^{99m}Tc -Cyt-PLGA-MPEG NP was increased to 16.6 times (20.02% ID) of the pure drug and 91 times grater in 24h.

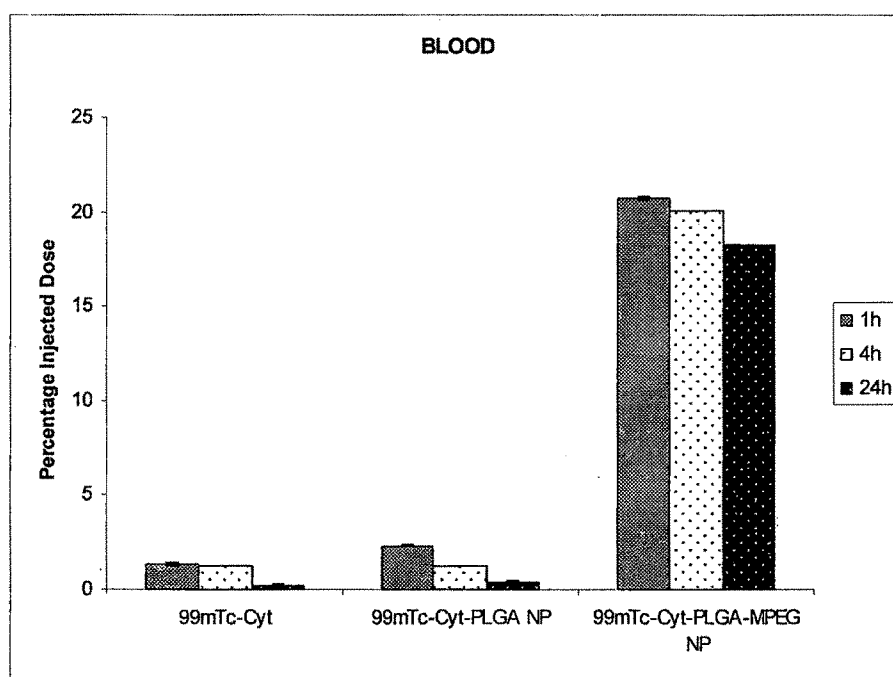


Fig. 7.10: Blood concentrations of ^{99m}Tc -Cyt-PLGA NP and ^{99m}Tc -Cyt-PLGA-mPEG NP in Balb/c mice at 1h, 4h and 24h interval post injection. Each value is the mean (\pm SD) of 3 mice

The biodistribution pattern of the two NP formulations was similar in heart, kidney, stomach, intestine and muscle. There was no significant difference ($p > 0.05$) between the two when compared to free drug.

Reduction in the uptake of the NPs was observed for the RES organs, Liver, spleen and lungs. The uptake ^{99m}Tc -Cyt-PLGA NP and ^{99m}Tc -Cyt-PLGA-mPEG NP by liver and spleen showed a significant difference ($p>0.05$) in their uptake compared to the free drug (^{99m}Tc -Cyt), the comparison of their uptake in terms of percentage of the ID is shown in Fig. 7.11a. In the liver the uptake of ^{99m}Tc -Cyt-PLGA NP was reduced by 3.1 times in 1h and 8.2 times in 4h. In the 24h the uptake of ^{99m}Tc -Cyt-PLGA NP was comparatively reduced by 1.5 times (2.86% ID) as that of free drug in liver. In the spleen the uptake of ^{99m}Tc -Cyt-PLGA NP was reduced by 4.0 times in 1h and 4.2 times in 4h. In the 24h the uptake of ^{99m}Tc -Cyt-PLGA NP was comparatively reduced by 1.2 times (3.0% ID) as that of free drug in spleen.

The uptake of ^{99m}Tc -Cyt-PLGA-MPEG NP was low initially for both liver and spleen (1.24% and 1.02% ID), which was gradually increased (2.02% and 2.08% ID) in 4h and finally the uptake of the NPs was reduced by both liver and spleen in 24h (0.71% and 1.23% ID respectively). Hence it was seen that there was a drastic reduction of uptake of ^{99m}Tc -Cyt-PLGA-MPEG NP by liver of about 11 times in 1 and 4h, and about 6 times reduction in 24h. A similar reduction pattern was seen in the uptake of ^{99m}Tc -Cyt-PLGA-MPEG NP by spleen, which was about 15.1 times reduction in 1h, 6.3 times in 4h and about 2.8 times lower than the pure drug.

Uptake by lungs is shown in Fig. 7.11b. There was a reduction of uptake by 1.4 times for ^{99m}Tc -Cyt-PLGA NP in 1 and 4h and nearly 1.8 times in 24h in the lungs. The reduction in uptake was much more prominent in case of ^{99m}Tc -Cyt-PLGA-MPEG NP, which was nearly 4 times (1.2% in 1h, 0.8% in 4h of ID) less than the pure drug in 1 and 4h. In 24h the reduction was further increased by 5.5 times (0.6% of ID) for ^{99m}Tc -Eto-PLGA-MPEG NP as compared to free drug (^{99m}Tc -Cyt) in lungs. The results clearly indicate that the uptake by the lungs has been reduced for PLGA NP and drastically reduced for PLGA-MPEG NP in the lungs, which shows that these NPs would remain in the blood circulation for a longer duration as also evident by their higher concentrations in the blood.

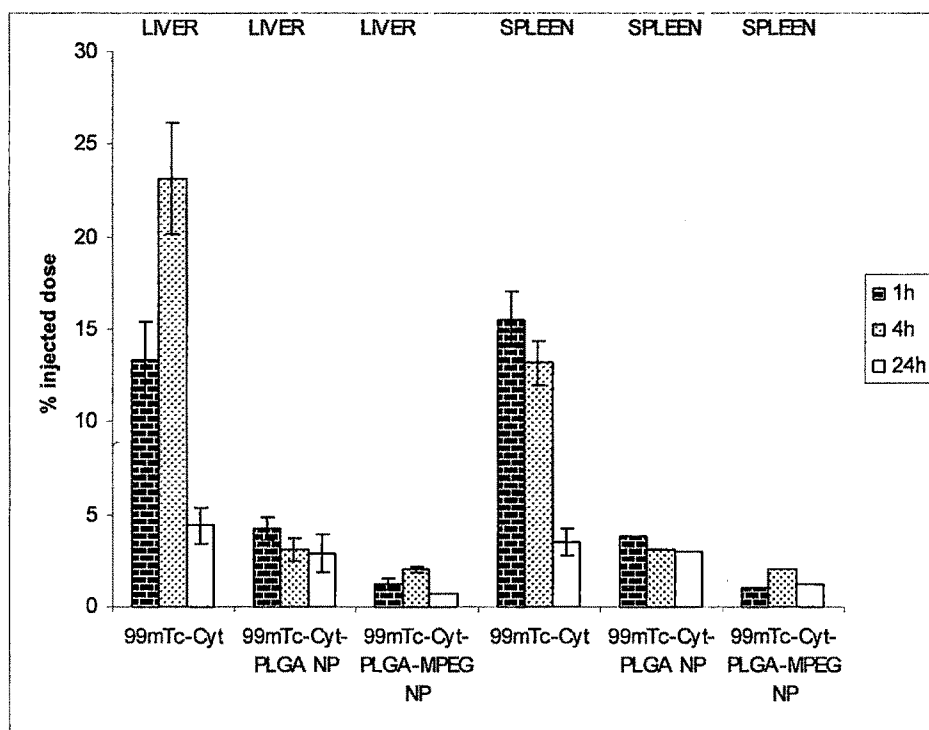


Fig. 7.11a: Liver and Spleen concentrations of ^{99m}Tc -Cyt-PLGA NP and ^{99m}Tc -Cyt-PLGA-mPEG NP in Balb/c mice at 1h, 4h and 24h interval post injection. Each value is the mean (\pm SD) of 3 mice

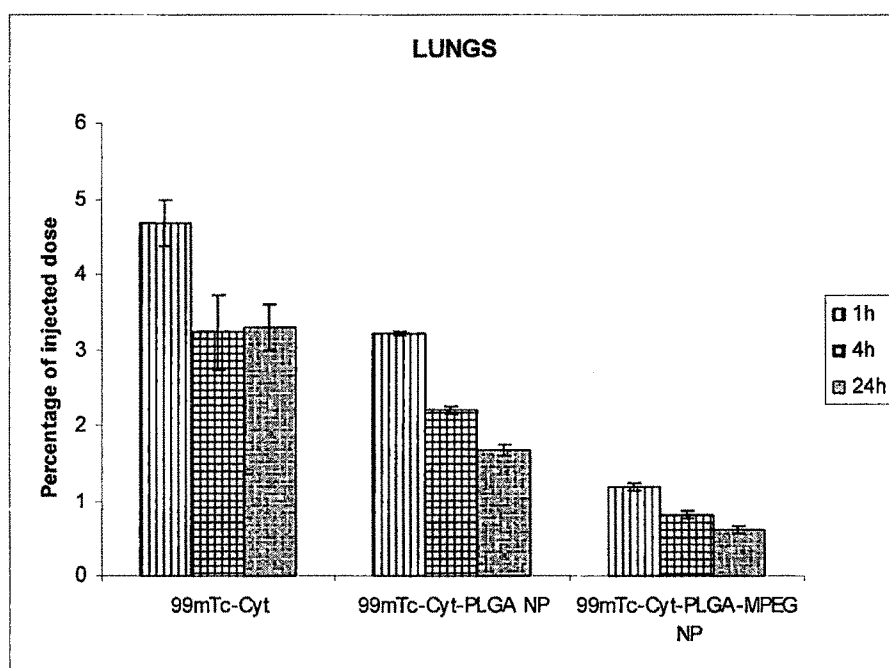


Fig. 7.11b: Lung concentrations of ^{99m}Tc -Cyt-PLGA NP and ^{99m}Tc -Cyt-PLGA-mPEG NP in Balb/c mice at 1h, 4h and 24h interval post injection. Each value is the mean (\pm SD) of 3 mice

There was no significant difference ($p < 0.05$) in the uptake of $^{99m}\text{Tc-Cyt}$ and $^{99m}\text{Tc-Cyt-PLGA NP}$ in the brain (Fig. 7.12). This indicates that the conventional PLGA NPs were not able to cross the blood brain barrier of the mice and were therefore not able to increase the concentration of cytarabine in the brain. Contrast to this, there was a significant difference ($p > 0.05$) in the biodistribution pattern of pegylated NPs of cytarabine, which showed drastic increase in the concentration of the NPs in the mice brain as compared to free drug. In the first hour the concentration of $^{99m}\text{Tc-Cyt-PLGA-MPEG NP}$ in the brain was 0.12% ID, which was about 3 times more than that of the free drug. Whereas the concentration of $^{99m}\text{Tc-Cyt-PLGA-MPEG NP}$ in brain was increase with time and was 1.24% ID making it about 25 times more than the pure drug in 4h. Similarly in 24h the uptake was further increased and was 1.62% ID, which was 23 times more than the pure drug.

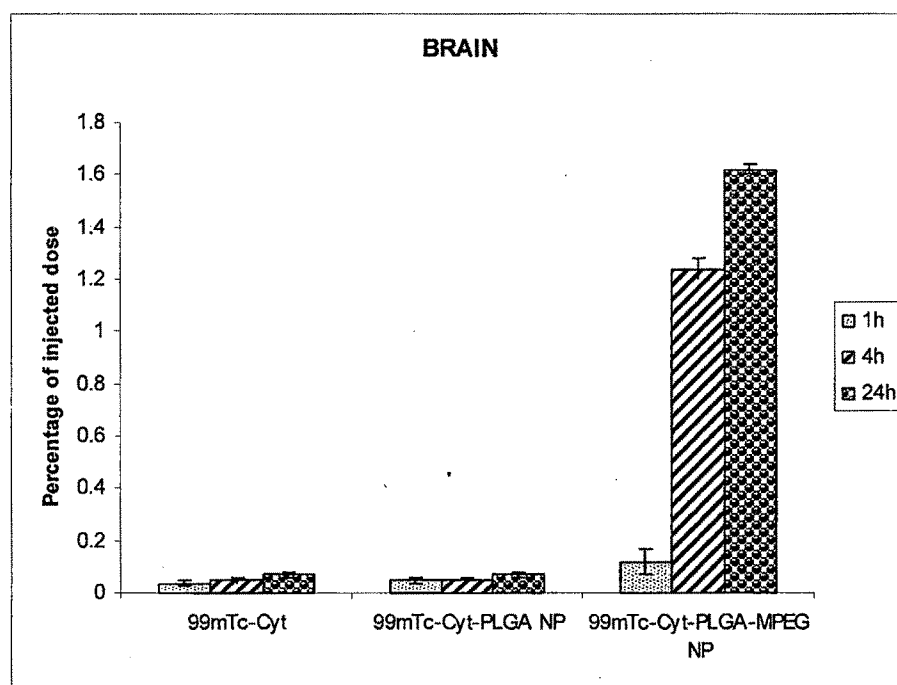


Fig. 7.12: Brain concentrations of $^{99m}\text{Tc-Cyt-PLGA NP}$ and $^{99m}\text{Tc-Cyt-PLGA-mPEG NP}$ in Balb/c mice at 1h, 4h and 24h interval post injection. Each value is the mean (\pm SD) of 3 mice

There was a significant difference in the uptake of both the NPs (^{99m}Tc -Cyt-PLGA NP and ^{99m}Tc -Cyt-PLGA-MPEG NP) compared to pure drug (^{99m}Tc -Cyt) and also among themselves in the bones (Fig. 7.13). The pattern followed for ^{99m}Tc -Cyt-PLGA-MPEG NP and ^{99m}Tc -Cyt was a decrease in concentration with time whereas the concentration of ^{99m}Tc -Cyt-PLGA NP decreased with time. The concentration of uptake of both the NPs was higher than the free drug, although the uptake of ^{99m}Tc -Cyt-PLGA-MPEG NP was much higher (6.5 times in 24h) than ^{99m}Tc -Cyt-PLGA NP. There was an increase in the uptake of ^{99m}Tc -Cyt-PLGA NP by 2.6 times (0.21% of ID) and 1.6 times (0.15% of ID) in 1 and 4h respectively compared to free drug ^{99m}Tc -Cyt in Femur bone. But in 24h the uptake of ^{99m}Tc -Cyt was more (0.12% ID) than that of ^{99m}Tc -Cyt-PLGA NP (0.08% ID). There was an increase in the uptake of ^{99m}Tc -Cyt-PLGA-MPEG NP by 2.2 times (0.18% ID), 5.4 times (0.49% of ID) and 4.3 times (0.52% of ID) in 1, 4 and 24h respectively compared to free drug ^{99m}Tc -Cyt in Femur bone of the mice.

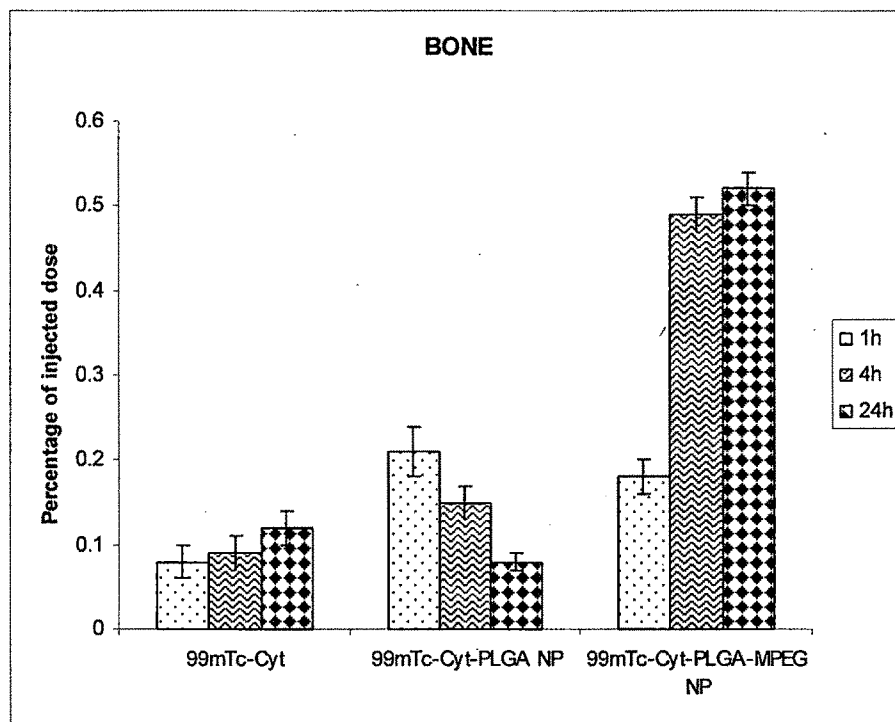


Fig. 7.13: Bone concentrations of ^{99m}Tc -Cyt-PLGA NP and ^{99m}Tc -Cyt-PLGA-mPEG NP in Balb/c mice at 1h, 4h and 24h interval post injection. Each value is the mean (\pm SD) of 3 mice

Conclusion

There was a great difference in the biodistribution pattern of the two NP formulations. The markedly increased blood circulation time and reduced liver uptake of the pegylated PLGA nanoparticles after i.v. administration to mice or rats compared to the non-pegylated nanoparticles has been demonstrated (Gref et al., 1994; Stolnik et al., 1994; After intravenous administration, the PLGA-PEG nanoparticles remain in the systemic circulation for hours, whereas the PLGA nanoparticles are removed from blood within few minutes.

^{99m}Tc -Cyt-PLGA NP was available at a very low concentration in blood compared to ^{99m}Tc -Cyt-PLGA-mPEG NP and was not able to avoid RES uptake. Moreover the distribution pattern of ^{99m}Tc -Cyt-PLGA NP was similar to that of the pure drug ^{99m}Tc -Cyt except for the fact that PLGA NP was available at a lower concentration in liver than the pure drug. The reason behind this could be that the PLGA-NP is expected to have more of splenic than hepatic clearance (Illum and Davis, 1984)

It was seen that ^{99m}Tc -Cyt-PLGA-mPEG NP was long circulating and its blood concentration was increased to 91.0 times in 24h compared to free drug. Comparatively, ^{99m}Tc -Cyt-PLGA NP was available in blood at a very low concentration and was almost negligible after 4h, this was probably due to its higher uptake by the liver and spleen. It has been reported that PEG-PLGA nanoparticles were in the blood at a much higher concentration than non-coated PLGA nanoparticles, which were accumulate in the liver and spleen when injected into BALB/c mice (Gref et al., 1994).

The pure drug (^{99m}Tc -Cyt) had negligible uptake by in the brain. ^{99m}Tc -Cyt-PLGA-mPEG NP was seen in a concentration 25 times that of ^{99m}Tc -Cyt-PLGA NP. Our results are in agreement with Brigger et al. (2002), who showed that PEGylated nanoparticles accumulated in the brain at a 4–8 fold higher concentration than non-PEGylated nanoparticles after intravenous injection into rats.

It was concluded that ^{99m}Tc -Cyt-PLGA-mPEG NP was present in blood in higher concentrations upto 24h, avoided RES uptake and was available in brain and bones.

SECTION C- BLOOD CLEARANCE STUDIES

7.10 Blood Clearance studies in Rats

Sprague-Dawley rats of either sex weighing 200 to 250 g were selected for the blood clearance studies. Into the tail vein of rats, nanoparticles containing 200 μCi of $^{99\text{m}}\text{Tc}$ were intravenously injected. The blood samples were collected at 15 minute, 30 minutes, 1 hour, 2 hours, 4 hours and 24 hours from the retro-orbital plexus of rat eye and analyzed for the radioactivity in gamma ray spectrometer. The blood was weighed, and radioactivity in whole blood was calculated by considering the volume of blood as 7.5% of the total body weight.

7.11 Results and Discussion

7.11.1 Blood Clearance of Etoposide and Etoposide loaded Nanoparticles

The blood clearance profile of $^{99\text{m}}\text{Tc}$ - Eto, $^{99\text{m}}\text{Tc}$ -Eto-PLGA NP₁₀₅, $^{99\text{m}}\text{Tc}$ - Eto-PLGA NP₁₆₀ and $^{99\text{m}}\text{Tc}$ - Eto-PLGA-mPEG NP in Rats is shown in Table 7.13 and Fig7.14. When $^{99\text{m}}\text{Tc}$ -Eto were injected in rat, only 2.35 %ID was seen in 15min, which was further decreased to 2.12 and 1.57 in 30min and 1h. Finally in 24h, only 0.05% ID was seen, indicating rapid elimination of ETO from the blood circulation. Among the three NPs, $^{99\text{m}}\text{Tc}$ - Eto-PLGA NP₁₆₀ concentration was reduced from 3.20% ID (15min) to 1.01% in 1h and 0.42% ID in 24h. The probable reason behind the fast elimination of $^{99\text{m}}\text{Tc}$ - Eto-PLGA NP₁₆₀ was attributed to its uncoated surface. Bazile et al. (1995) have reported that uncoated nanoparticles were rapidly removed from the circulation due to their uptake by the macrophages in the liver, spleen and lungs.

$^{99\text{m}}\text{Tc}$ -Eto-PLGA NP₁₀₅ was present in higher concentrations (15.38% of ID) in the blood upto 24h. This was probably due to the fact that nanoparticles of size less than 100 nm diameter can evade the RES and have a long circulation time in the blood (Gaur et al., 2000). Particles with hydrodynamic radii of over 200 nm typically exhibit a more rapid rate of clearance than particles with radii under 200 nm, regardless of whether they are PEGylated or not (Moghimi et al., 1993). In other words, a 150 nm nanoparticle would be cleared from the blood stream much more rapidly than a 70 nm particle. Similarly in our case, $^{99\text{m}}\text{Tc}$ -Eto-PLGA NP₁₀₅ (MPS 105nm) remained in the circulation for a longer duration than $^{99\text{m}}\text{Tc}$ - Eto-PLGA NP₁₆₀ (MPS 160nm).

Table 7.13
Blood clearance of ^{99m}Tc - Eto, ^{99m}Tc -Eto-PLGA NP₁₀₅, ^{99m}Tc - Eto-PLGA NP₁₆₀, ^{99m}Tc -Eto-PLGA-PLU NP and ^{99m}Tc - Eto-PLGA- mPEG NP in Rats

Time	Percentage Injected Dose in blood											
	^{99m}Tc -Eto		^{99m}Tc -Eto-PLGA NP ₁₀₅		^{99m}Tc - Eto-PLGA NP ₁₆₀		^{99m}Tc -Eto-PLGA- PLU NP		^{99m}Tc -Eto-PLGA- mPEG NP			
	Mean	SD	Mean	SD	Mean	SD	Mean	SD	Mean	SD		
15min	2.35	0.08	33.20	0.75	3.20	0.05	40.91	1.83	37.39	2.08		
30min	2.12	0.04	31.23	0.82	1.63	0.02	38.35	1.15	35.21	3.25		
1h	1.57	0.03	24.26	0.60	1.01	0.04	22.10	1.20	30.20	1.38		
2h	0.89	0.23	19.94	0.50	0.85	0.08	21.20	1.52	28.20	2.50		
4h	0.53	0.08	17.03	0.70	0.73	0.12	19.14	1.61	21.18	1.70		
24h	0.05	0.01	15.38	0.90	0.42	0.06	16.31	1.50	18.30	1.20		

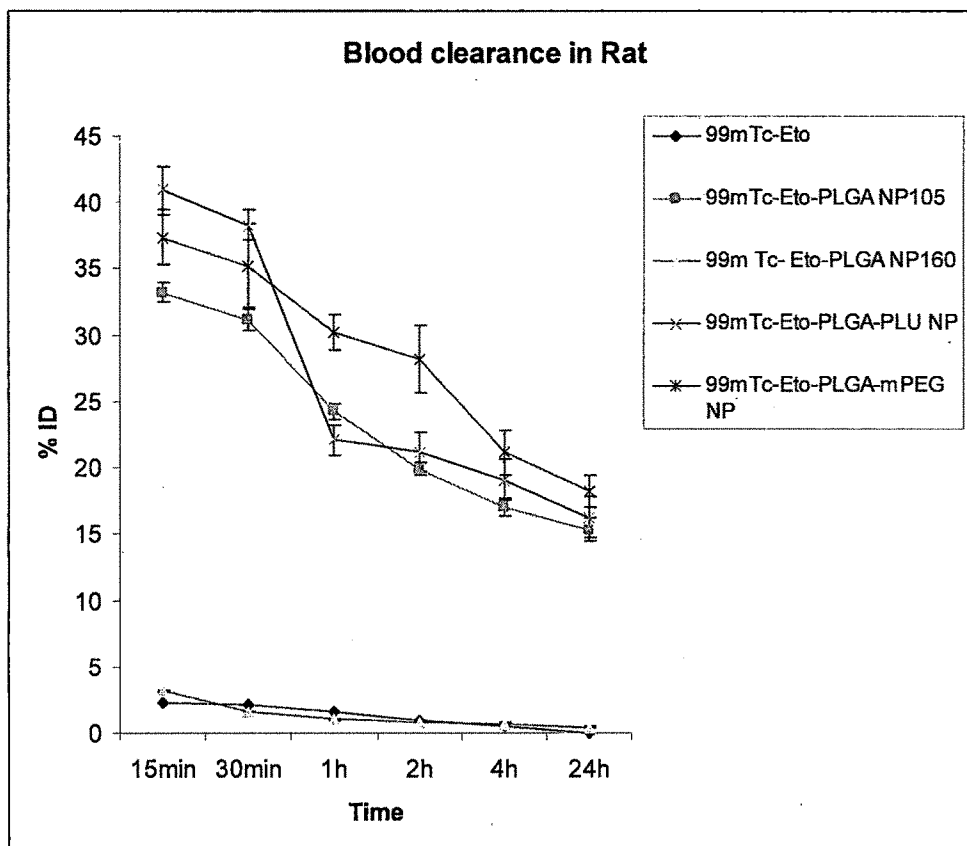


Fig 7.14: Blood clearance of $^{99m}\text{Tc-Eto}$, $^{99m}\text{Tc-Eto-PLGA NP}_{105}$, $^{99m}\text{Tc-Eto-PLGA NP}_{160}$ and $^{99m}\text{Tc-Eto-PLGA-mPEG NP}$ in Rats

The two coated NPs, $^{99m}\text{Tc-Eto-PLGA-PLU NP}$ and $^{99m}\text{Tc-Eto-PLGA-mPEG NP}$ were available in higher concentrations in the circulation compared to the pure drug and among the two, $^{99m}\text{Tc-Eto-PLGA-mPEG NP}$ had the higher value of 18.30% ID at 24h. This was probably due to the fact that Pluronic coated NP are faster eliminated compared to MPEG coated NP (Storm et al., 1995)

Hence it was concluded that $^{99m}\text{Tc-Eto-PLGA-mPEG NP}$ was present in the blood at higher concentrations upto 24h.

7.11.2 Blood Clearance of cytarabine and cytarabine loaded Nanoparticles

The blood clearance profile of ^{99m}Tc - Cyt, ^{99m}Tc - Cyt,-PLGA NP and ^{99m}Tc - Cyt-PLGA-mPEG NP in Rats is shown in Table 7.14 and Fig7.15. When ^{99m}Tc -Cyt were injected in rat, only 2.35 %ID was seen in 15min, which was further decreased to 3.24 and 2.36 in 30min and 1h. In the 2h the concentration was further reduced to 1.23% ID, only a fraction of 0.07% ID was seen in 24h. Similarly ^{99m}Tc - Cyt-PLGA NP was also only seen in small concentration of 2.15% in 1h and was further reduced to 0.21% ID in 24h, indicating convention NP, which were not surface modified were rapidly eliminated from the blood circulation. Whereas ^{99m}Tc -Cyt-PLGA-MPEG was seen in higher concentrations in blood upto 24h. The blood concentration of ^{99m}Tc - Cyt-PLGA-MPEG NP was 32.25% ID in 15 min and 12.27 in 24h.

Table 7.14
Blood clearance of ^{99m}Tc -Cyt, ^{99m}Tc -Cyt-PLGA NP and ^{99m}Tc - CYT-PLGA NP in Rats

Time	Percentage Injected Dose in blood					
	^{99m}Tc -Cyt		^{99m}Tc -Cyt-PLGA NP		^{99m}Tc -Cyt-PLGA-mPEG NP	
	Mean	SD	Mean	SD	Mean	SD
15 min	4.21	0.12	2.15	0.08	32.25	3.75
30 min	3.24	0.08	1.02	0.06	28.25	3.82
1 hr	2.36	0.03	0.82	0.05	24.21	2.60
2hr	1.23	0.25	0.61	0.25	18.29	3.50
4hr	1.05	0.07	0.40	0.09	15.20	2.70
24hr	0.07	0.02	0.21	0.06	12.27	1.10

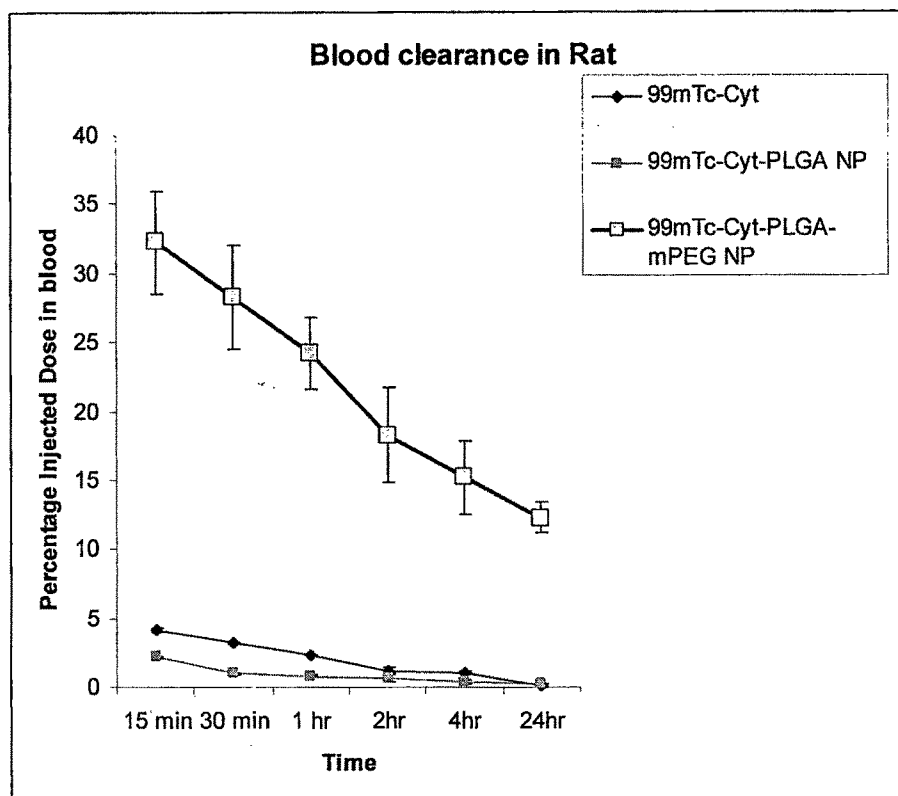


Fig 7.15: Blood clearance of $^{99m}\text{Tc-Cyt}$, $^{99m}\text{Tc-Cyt-PLGA NP}$ and $^{99m}\text{Tc-Cyt-PLGA-mPEG NP}$ in Rats

The results indicated that only PEGylated NP of CYT could sustain the release in higher concentrations in the rats, whereas pure drug and PLGA NP were almost eliminated after the 4th hour. It has been shown that PLGA nanoparticles (non-coated) when injected into mice accumulate in the liver and spleen, whereas PEG-PLGA nanoparticles remain in the circulation at higher concentrations Gref et al., (1994).

The study concluded that PEGylated nanoparticles of CYT, $^{99m}\text{Tc-Cyt-PLGA-mPEG NP}$ was present at higher concentrations in rat circulation upto 24h.

REFERENCES

- Banerjee T, Singh AK, Sharma RK, Maitra AN (2005). Labeling efficiency and biodistribution of Technetium-99m labeled nanoparticles: interference by colloidal tin oxide particles. *International Journal of Pharmaceutics* 289, 189–195.
- Banerjee S, Pillai MR, Ramamoorthy N (2001). Evolution of Tc-99m in diagnostic radiopharmaceuticals. *Seminars in Nuclear Medicine* 31, 260–277.
- Brigger I, Dubernet C, Couvreur P (2002). Nanoparticles in cancer therapy and diagnosis. *Advanced Drug Delivery Reviews* 54, 631–651.
- Brigger I, Morizet J, Laudani L, Aubert G, Appel M, Velasco V, Terrier-Lacombe MJ, Desmaele D, D'Angelo J, Couvreur P, Vassal G (2004). Negative preclinical results with stealth® nanospheres-encapsulated doxorubicin in an orthotopic murine brain tumor model. *Journal of Controlled Release* 100, 29–40.
- Chiannilkulchai N, Ammoury N, Caillou B, Devissaguet JP, Couvreur P (1990). Hepatic tissue distribution of doxorubicin-loaded nanoparticles after, I.V. administration in reticulosarcoma M 5076 metastases-bearing mice. *Cancer Chemotherapy and Pharmacology* 26, 122–126.
- Coleman RE (2003). Radionuclide Imaging in Cancer Medicine. Cancer Imaging. Cancer in Medicine, American Cancer Society.
- Davis SS, Douglas SJ, Illum L, Jones PDE, Mak E, Muller RH (1986). Targeting of colloidal carriers and the role of surface properties. In: G. Gregoriadis J, Senior and G. Poste (Eds.). Targeting of Drugs with Synthetic Systems. NATO ASI Series Vol. 113, Plenum Press, New York, pp. 123-146.
- Davis SS and Illum L (1988). Polymeric microspheres as drug carriers. *Biomaterials* 9, 110I-1115.
- Dietlein M, Pels H, Schulz H, Staak O, Borchmann P, Schomacker K, Fischer T, Eschner W, Pogge von Strandmann E, Schicha H, Engert A, Schnell R (2005). Imaging of central nervous system lymphomas with iodine-123 labeled rituximab. *European Journal of Haematology* 74 (4), 348–352.
- Douglas SJ, Davis SS, Illum I (1986). Biodistribution of poly(butyl 2-cyanoacrylate) nanoparticles in rabbits. *International Journal of Pharmaceutics* 34, 145-152.
- Garnett MC, Kallinteri P (2006). Nanomedicines and nanotoxicology: some physiological principles. *Occup. Med. (London)* 56 (5), 307–311.

Gaur U, Sahoo SK, De TK, Maitra AN, Ghosh PC, Ghosh PK (2000). Biodistribution of fluoresceinated dextran using novel nanoparticles evading reticuloendothelial system. *International Journal of Pharmaceutics* 202, 1–10.

Ghanem GE, Joubran C, Arnould R, Lejeune F, Fruhling J (1993). Labelled polycyanoacrylate nanoparticles for human in vivo use, *Appl. Radiat. Isot.* 44 (9), 1219–1224.

Gref R, Minamitake Y, Peracchia V, Trubetskoy V, Torchillin V, Langer R (1994). Biodegradable long-circulating polymeric microspheres. *Science* 263, 1600–1603.

Hagens WI, Oomen AG, de Jong WH, Cassee FR, Sips AJ (2007) What do we (need to) know about the kinetic properties of nanoparticles in the body? *Regul. Toxicol. Pharmacol.* 49 (3), 217–219.

Hamoudeh M, Kamleh MA, Diab R, Fessi H (2008). Radionuclides delivery systems for nuclear imaging and radiotherapy of cancer. *Advanced Drug Delivery Reviews* 60, 1329–1346.

Illum L and Davis SS (1983). Effect of the nonionic surfactant poloxamer 338 on the fate and deposition of polystyrene microspheres following intravenous administration. *Journal of Pharmaceutical Sciences* 72, 1086-1089.

Illum L and Davis SS (1984). The organ uptake of Intravenously administered colloidal particles can be altered using a non-ionic surfactant (poloxamer 338). *FEBS Letters* 167, 79-82.

Juliano RL (1988). Factors affecting the clearance kinetics and tissue distribution of liposomes, microspheres and emulsions. *Advanced Drug Delivery Reviews* 2, 31- 54.

Kocbek P, Obermajer N, Cegnar M, Kos J, Kristl J (2007). Targeting cancer cells using PLGA nanoparticles surface modified with monoclonal antibody. *Journal of Controlled Release* 120, 18–26.

Moghimi SM and Davis SS (1994). Innovations in avoiding particle clearance from blood by Kupffer cells: some cause for reflection. *Critical Reviews in Therapeutic Drug Carrier Systems* 11, 31-59.

Moghimi SM, Hunter AC, Murray JC (2005). Nanomedicine: current status and future prospects. *FASEB Journal* 19 (3), 311–330.

Reddy LH, Sharma RK, Chuttani K, Mishra AK, Murthy RR (2004). Etoposide incorporated tripalmitin nanoparticles with different surface charge: formulation, characterization, radiolabeling, and biodistribution studies. *AAPS Journal* 6 (3), e23

Chapter7- Radiolabeling, Biodistribution and Blood Clearance studies

Stella B, Arpicco S, Peracchia MT, Desmaële D, Hoebeke J, Renoir M, D'Angelo J, Cattel L, Couvreur P, (2000). Design of folic acid-conjugated nanoparticles for drug targeting. *Journal of Pharmaceutical Sciences* 89 (11), 1452–1464.

Storm G, Belliot SO, Daemen T, Lasic DD (1995). Surface modification of nanoparticles to oppose uptake by mononuclear phagocyte system. *Advanced Drug Delivery Reviews* 17, 31–48.

Theobald AE (1990). Text book of radiopharmacy: theory and practice In: Sampson CB Ed, New York, Gordan and Breach, 127-129.